

Adaptive Processing of SAR Data for ATR

Mehrdad Soumekh

M. Soumekh Consultant &
Department of Electrical Engineering
332 Bonner Hall, SUNY-Buffalo
Amherst, NY 14260
Phone: (716) 645-3115 x 2138
Email: msoum@eng.buffalo.edu

1. Introduction

In this presentation, we outline a framework for Automatic Target Recognition (ATR) in Synthetic Aperture Radar (SAR) that is based on an adaptive processing of the *digitally-spotlighted* phase history data of individual targets. In the conventional SAR-ATR algorithms, the magnitude only or the complex SAR image of a *test* target chip is analyzed and compared with a set of *reference* target chips to determine the test target type or class. Depending on the relative coordinates of a test target in the imaging scene and the flight path of the radar-carrying aircraft, the SAR image (chip) of the test target possesses a spatial warping with respect to the reference target chips that should be *blindly* incorporated and/or compensated in the ATR algorithm. Furthermore, the formed SAR images exhibit certain (slant plane) parametric variations and erroneous shifts that depend on the type of the SAR imaging algorithm that is used. For the success of a SAR-ATR algorithm, the spatial warping and slant plane parameters of the SAR imaging algorithm should be available to the user. In practice, these parameters of the formed SAR image are not exactly known to the SAR-ATR user.

Moreover, any comparison between the test and reference target chips requires understanding and incorporating the sensor and platform variations in the corresponding SAR data acquisitions. The sensor variations are caused by various subtle changes (imperfections) in the radar system circuitry (e.g., waveform generator, cables, etc.), and undesirable amplitude/phase fluctuations in the radiation pattern of the physical radar between the reference and test data collections; these are unknown and result in different *2D Image Point Response* (IPR) or *Point Spread Function* (PSF) in the reference and test SAR images. The above-mentioned ambiguities result in unknown subtle geometric distortions and complex PSF variations in the reconstructed SAR image that have adverse effects on the performance of any SAR-ATR algorithm.

Report Documentation Page

*Form Approved
OMB No. 0704-0188*

Public reporting burden for the collection of information is estimated to average 1 hour per response, including the time for reviewing instructions, searching existing data sources, gathering and maintaining the data needed, and completing and reviewing the collection of information. Send comments regarding this burden estimate or any other aspect of this collection of information, including suggestions for reducing this burden, to Washington Headquarters Services, Directorate for Information Operations and Reports, 1215 Jefferson Davis Highway, Suite 1204, Arlington VA 22202-4302. Respondents should be aware that notwithstanding any other provision of law, no person shall be subject to a penalty for failing to comply with a collection of information if it does not display a currently valid OMB control number.

1. REPORT DATE 01 MAY 2005	2. REPORT TYPE N/A	3. DATES COVERED -			
4. TITLE AND SUBTITLE Adaptive Processing of SAR Data for ATR		5a. CONTRACT NUMBER			
		5b. GRANT NUMBER			
		5c. PROGRAM ELEMENT NUMBER			
6. AUTHOR(S)		5d. PROJECT NUMBER			
		5e. TASK NUMBER			
		5f. WORK UNIT NUMBER			
7. PERFORMING ORGANIZATION NAME(S) AND ADDRESS(ES) M. Soumekh Consultant & Department of Electrical Engineering 332 Bonner Hall, SUNY-Buffalo Amherst, NY 14260		8. PERFORMING ORGANIZATION REPORT NUMBER			
9. SPONSORING/MONITORING AGENCY NAME(S) AND ADDRESS(ES)		10. SPONSOR/MONITOR'S ACRONYM(S)			
		11. SPONSOR/MONITOR'S REPORT NUMBER(S)			
12. DISTRIBUTION/AVAILABILITY STATEMENT Approved for public release, distribution unlimited					
13. SUPPLEMENTARY NOTES See also ADM202152., The original document contains color images.					
14. ABSTRACT					
15. SUBJECT TERMS					
16. SECURITY CLASSIFICATION OF:			17. LIMITATION OF ABSTRACT UU	18. NUMBER OF PAGES 58	19a. NAME OF RESPONSIBLE PERSON
a. REPORT unclassified	b. ABSTRACT unclassified	c. THIS PAGE unclassified			

Adaptive Processing of SAR Data for ATR

In this work, we provide a two-stage SAR-ATR algorithm that is not sensitive to the above-mentioned problems. In the proposed approach, the SAR-ATR user applies a relatively fast CFAR detection algorithm with a high probability of false alarm as well as a high probability of detection to identify the coordinates of suspected targets in a SAR imaging scene. Next, the coordinates of each suspected target is passed to what we refer to as the *digital-spotlighting* algorithm that extracts the SAR phase history data of a neighborhood within the input coordinates. The resultant database is the complex SAR signature (phase history) of the chip area at the desired coordinates that carries information on the variations of the target's complex radar signature with respect to the fast-time (radar) frequency and aspect angle. This database is then compared with a set of reference phase history models to identify the target at the input coordinates where the original ATR algorithm detected a suspected target.

A 2D *adaptive* method for the above-mentioned matching of test and reference phase history data is utilized, an algorithm that we call *signal subspace matched filtering*, that is not sensitive to the calibration errors of the SAR system (i.e., variations of the radar radiation pattern from one experiment to another). Such calibration errors, that could drastically alter the *phase* information of a target's SAR signature, are one of the major obstacles in exploiting the *complex* SAR signature of a target in the classification/recognition problems. The signal subspace processing method performs a *blind calibration* of variations of the IPRs of the reference and test SAR phase history data using 2D adaptive filtering methods. This calibration also compensates for variations in the IPRs that are due to imperfect (errors in) motion data and required 2D auto-focusing to compensate for them (among other SAR system phase errors such as range-gate slip) that never results in the theoretical (ideal) SAR image.

2. Sources of Calibration Errors

SAR signature of a target depends on the radar sensor characteristics (beam pattern, signal generator, etc.) as well as the physical properties of the target. Figure 1 shows the overall system diagram for generation of a target signature in SAR. In SAR-ATR, comparison between the test and reference target chips requires understanding and incorporating the sensor and platform variations in the corresponding SAR data acquisitions. The sensor variations are caused by various subtle changes (imperfections) in the radar system circuitry (e.g., waveform generator, cables, etc.), and undesirable amplitude/phase fluctuations in the radiation pattern of the physical radar between the reference and test data collections; see Figures 2a and 2c. These are unknown and result in different 2D *Image Point Response* (IPR) or *Point Spread Function* (PSF) in the reference and test SAR images. These ambiguities result in unknown subtle geometric distortions and complex PSF variations in the reconstructed SAR image that have adverse effects on the performance of any SAR-ATR algorithm. Variations in the target may also exist; e.g., rotation in the gun of a tank, opening or closing of driver/commander/turret hatch, etc.; see Figure 2d.

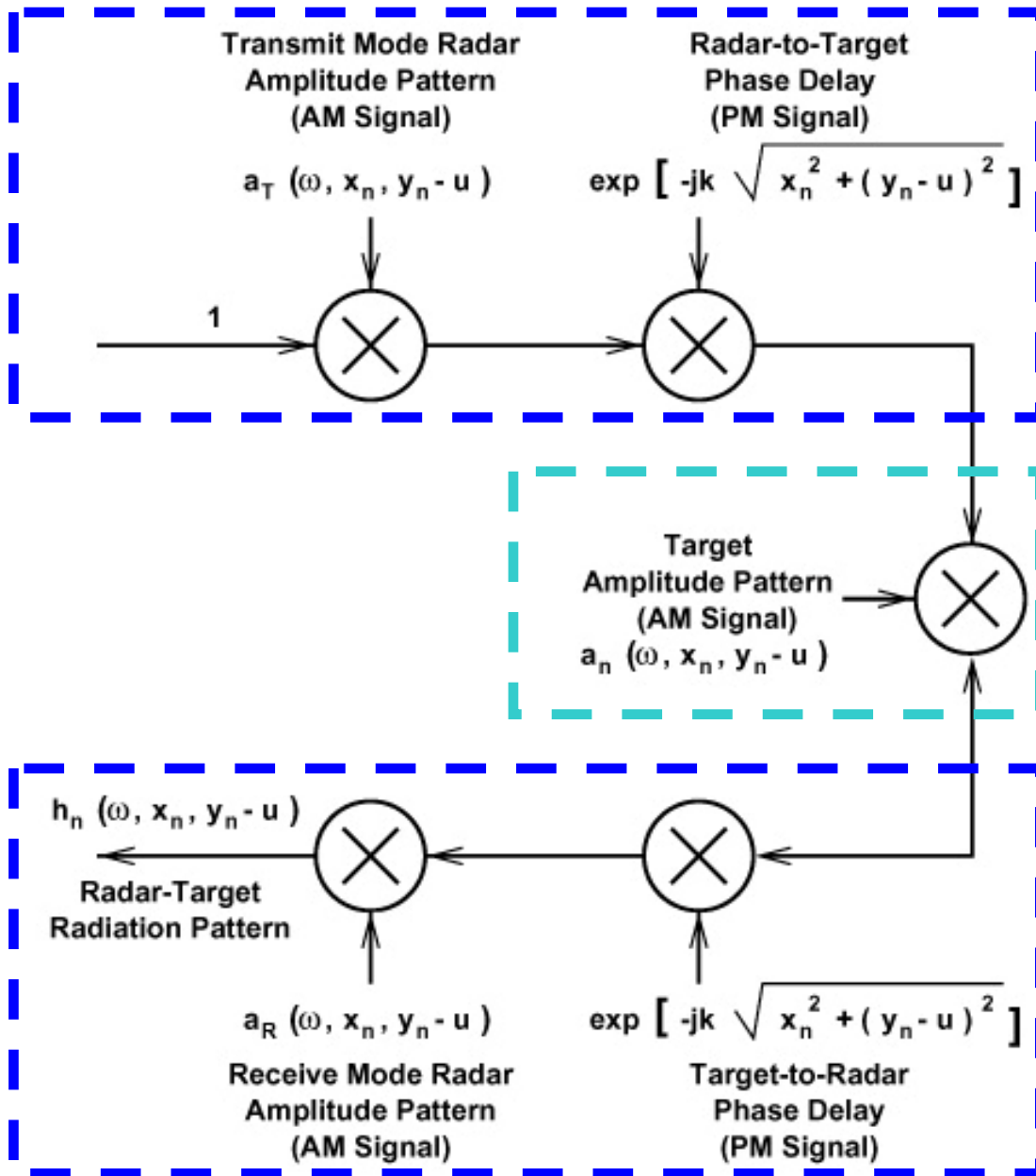


Figure 1. Model for Generation of SAR Signal

Variations in Radar Transmit-Mode Beam Pattern

Variations in Motion & Autofocus

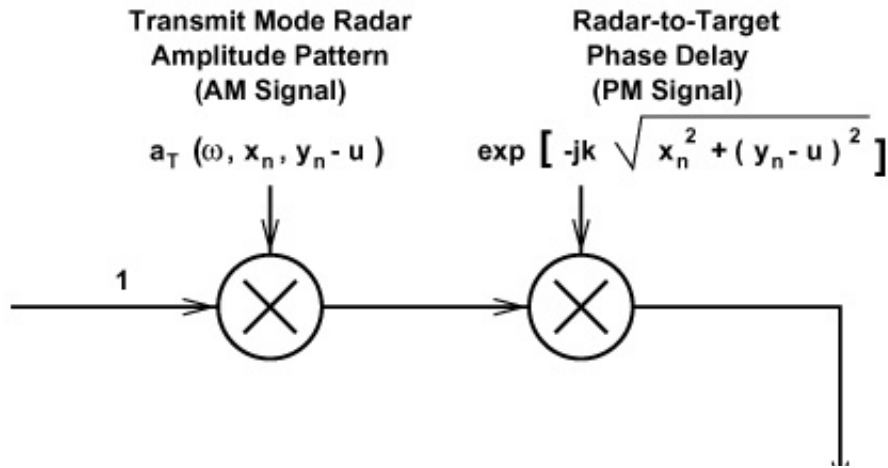


Figure 2a. SAR Calibration Errors: Transmit Mode

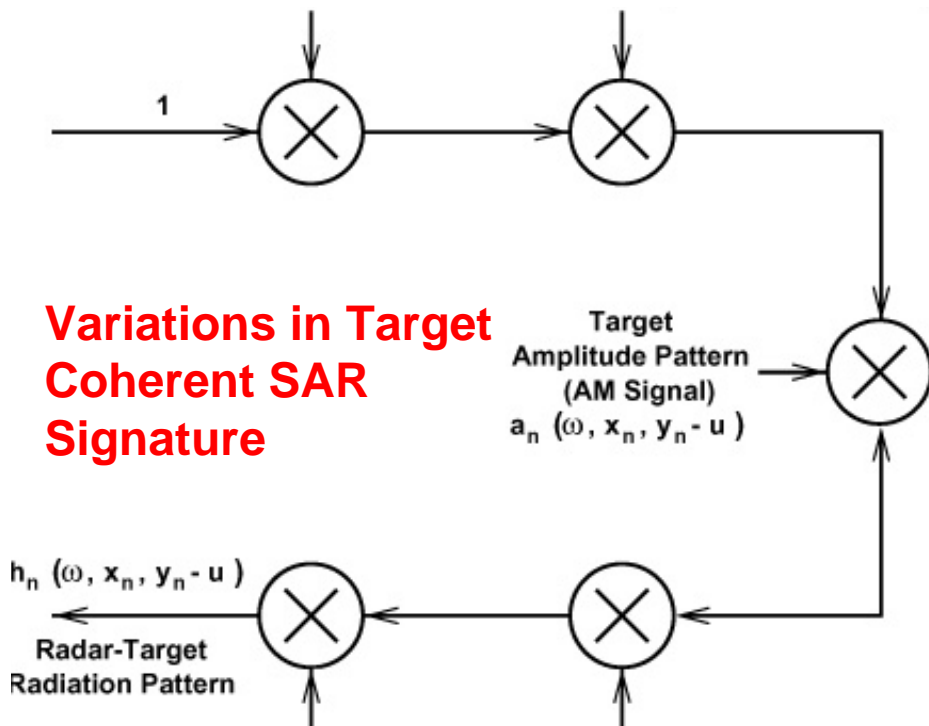
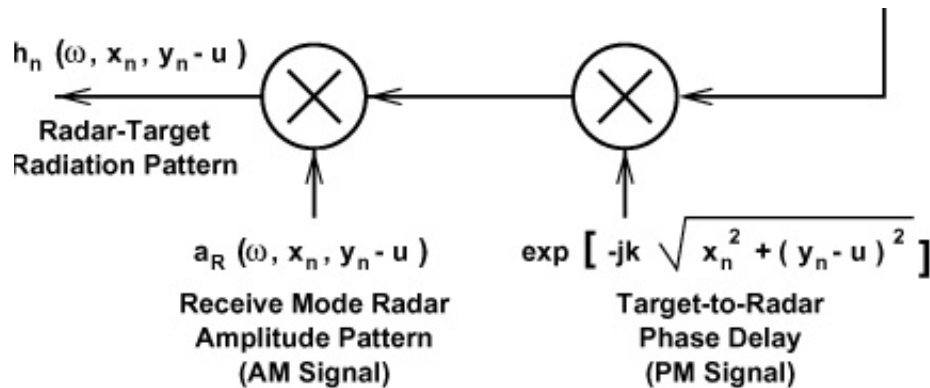


Figure 2b. SAR Calibration Errors: Variations in Target



**Variations in Radar
Receive-Mode
Beam Pattern**

**Variations in
Motion &
Autofocus**

Figure 2c. SAR Calibration Errors: Receive Mode

3. Adaptive Calibration of Dual SAR Imagery via Signal Subspace Processing

In SAR-ATR, the task of a signal processor is to blindly compensate for the above-mentioned calibration errors. For this purpose, we utilize a 2D *adaptive* method for the matching of test and reference target chips is utilized [1]. This algorithm, that we call *signal subspace matched filtering*, is not sensitive to the calibration errors of the SAR system (i.e., variations of the radar radiation pattern, etc. from one experiment to another) as well as small variations in the target. The mathematical foundation of this approach is the same as an adaptive filtering algorithm that we have developed for coherent change detection [2], [1, ch. 8], and moving target detection [1, ch. 8], [3], [4] in SAR systems.

The following outlines the foundation of the adaptive signal subspace algorithm using first a one-dimensional signal space. The results are then extended to the two-dimensional problems of SAR.

We can solve for each of the filter coefficients by calculating the inner product with the corresponding orthonormal basis vector:

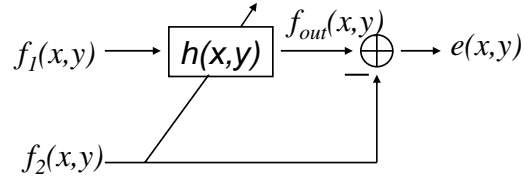
$$\begin{aligned}\hat{h}(i) &= \left\langle \hat{\mathbf{v}}_{-2}\hat{h}(-2) + \hat{\mathbf{v}}_{-1}\hat{h}(-1) + \hat{\mathbf{v}}_0\hat{h}(0) + \hat{\mathbf{v}}_1\hat{h}(1) + \hat{\mathbf{v}}_2\hat{h}(2), \hat{\mathbf{v}}_i \right\rangle \\ &= \left\langle \hat{\mathbf{v}}_i, \mathbf{v}_{out} \right\rangle\end{aligned}$$

These coefficients can then be used to calculate the projection of $f_2(x)$ signal into the signal subspace of $f_1(x)$.

→ The resulting output of $h(x)$ (the estimate of $f_2(x)$) is simply the projection of $f_2(x)$ into the signal subspace of $f_1(x)$!!

The difference between the reference signal and the projected test signal becomes: $e = \hat{f}_2 - f_1$
which also shows how much the test signal differs from the reference.

Extension to 2D



Linear Filter:

$$f_2^{(k)}(x_i, y_j) = \sum_{m=-n_x}^{n_x} \sum_{n=-n_y}^{n_y} h_{mn}^{(k)} f_1^{(k)}(x_i - m\Delta_x, y_j - n\Delta_y)$$

Signal Subspace:

$$\Phi_1^{(k)} = [f_1^{(k)}(x_i - m\Delta_x, y_j - n\Delta_y); m = -n_x, \dots, n_x, n = -n_y, \dots, n_y]$$

The orthonormalized Signal Subspace:

$$\Theta_1^{(k)} = [\theta_1^{(k)}(x_i - m\Delta_x, y_j - n\Delta_y); m = -n_x, \dots, n_x, n = -n_y, \dots, n_y, \\ x_i = x_{\min, k}, x_{\min, k} + 1, \dots, x_{\max, k}, \\ y_j = y_{\min, k}, y_{\min, k} + 1, \dots, y_{\max, k}]$$

The filter output (for the normalized subspace):

$$\hat{f}_2^{(k)}(x_i, y_j) = \sum_{m=-n_x}^{n_x} \sum_{n=-n_y}^{n_y} \hat{h}_{mn}^{(k)} f_1^{(k)}(x_i - m\Delta_x, y_j - n\Delta_y)$$

Analogous to the 1D case, the output of the filter is simply the projection of $f_2^{(k)}(x,y)$ into $\Theta^{(k)}$.

4. Adaptive SAR-ATR: Ka Band Turntable (ISAR) Data

We next examine the application of the SSP algorithm in SAR-ATR using a Ka band turntable ISAR database. Figure 3a shows a portion of the measured ISAR data in the radar frequency and aspect angle domain. The first issue that we notice for this database is the irregular vertical lines. Figure 3b shows the cumulative spectrum of the data. This indicates irregular transmitter power variations in the ISAR data.

This is also a calibration error source that can be easily compensated for using the inverse of the distribution in Figure 3b as a filter to be applied to the measured ISAR data. (Note that this is *magnitude* only calibration. One may also perform phase calibration provided an omni-directional target had been put in the imaging scene.) Figure 3c shows the magnitude-calibrated ISAR data.

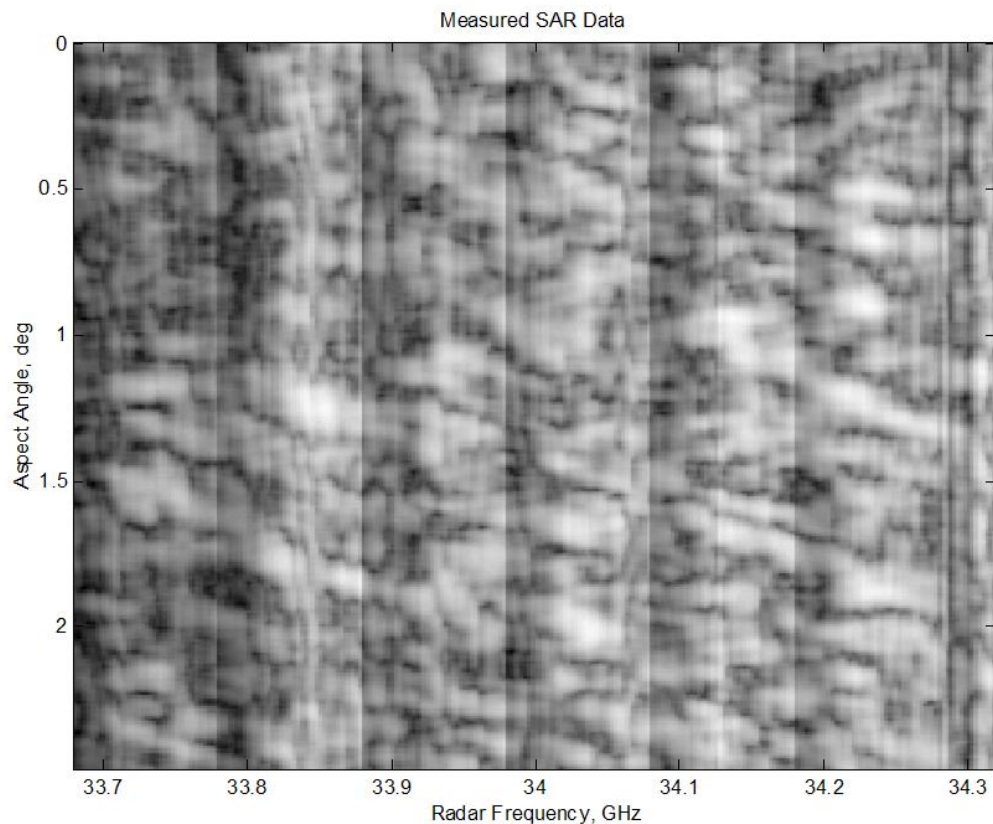


Figure 3a. Measured ISAR Data

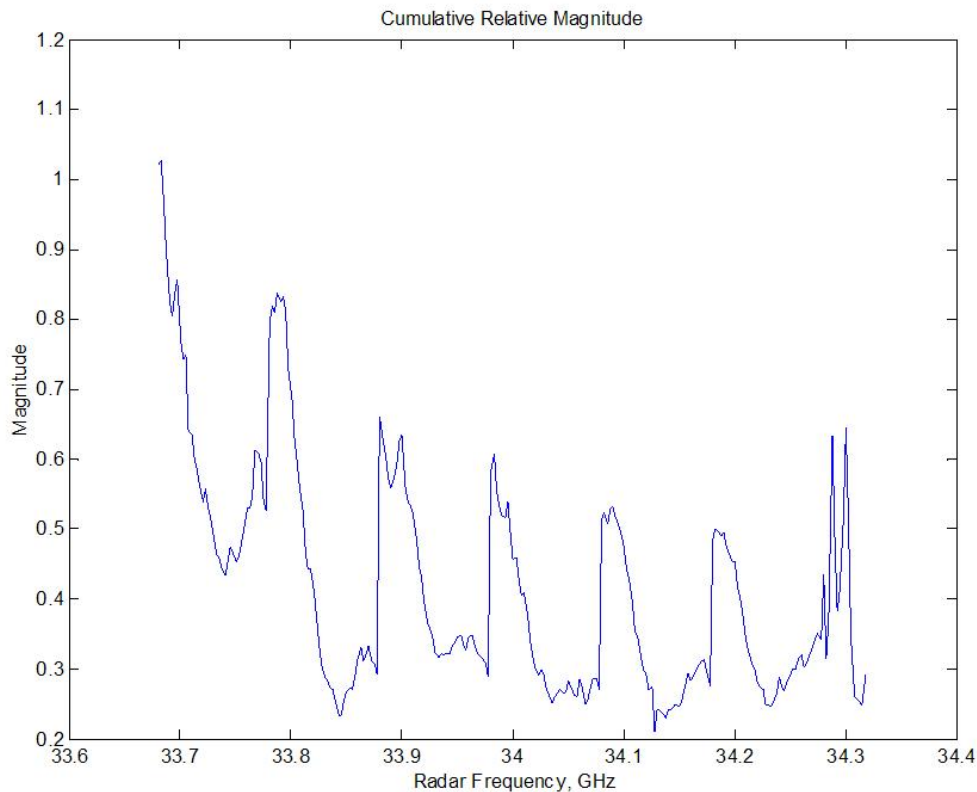


Figure 3b. Cumulative Spectrum of Measured ISAR Data

We use two SAR/ISAR reconstruction algorithms to form images from the magnitude-calibrated data. The first method is the polar format algorithm that is based on approximations; the second method is the wavefront reconstruction algorithm that is error-free [1, ch. 7]. Figures 4a and 4b are the resultant images using 16 degrees of integration angle; similar results for a 32-degree integration angle are shown in Figures 5a and 5b. Note that the wavefront reconstruction algorithm provides better images. For our SAR-ATR study, the wavefront images are used.

For the SAR-ATR study, we consider two of the ISAR databases of a T-72 tank: T06.frq and T07.frq. The difference between the two databases is the orientation of the gun of the vehicle: for the T06.frq data, the gun is at the azimuth angle of -20 degrees; the azimuth angle of the gun is zero for the T07.frq data. Thus, the recognition algorithm should match the structure of the T-72 tank, except for the gun, in the two databases.

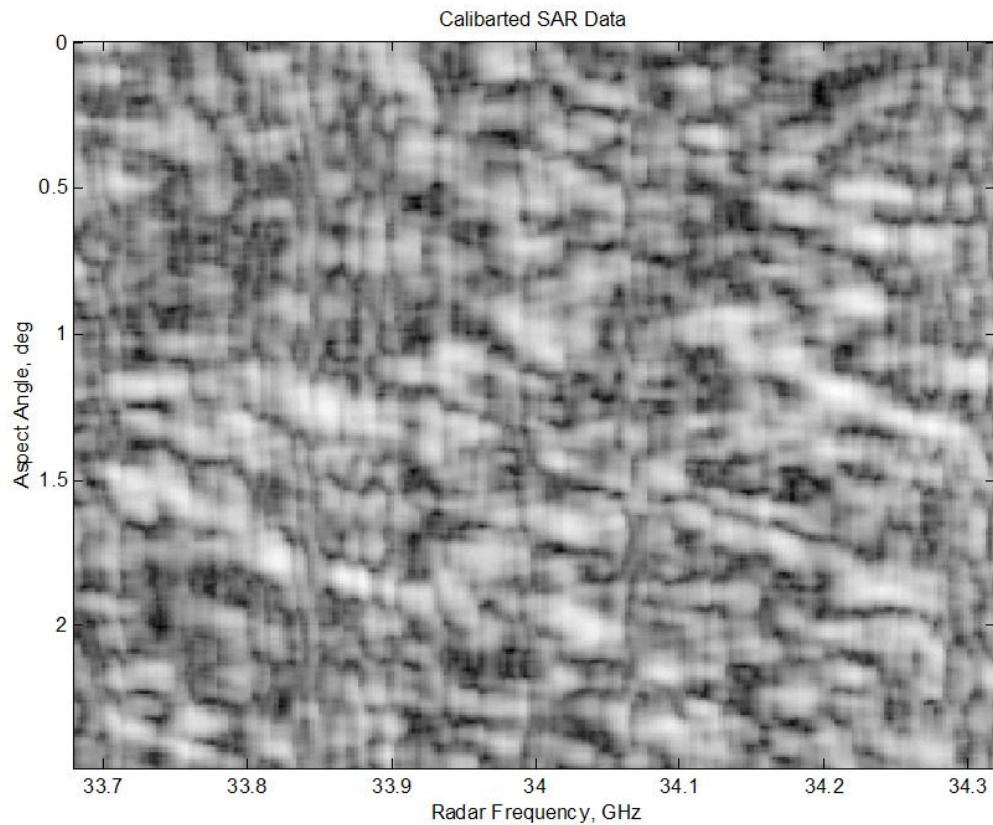
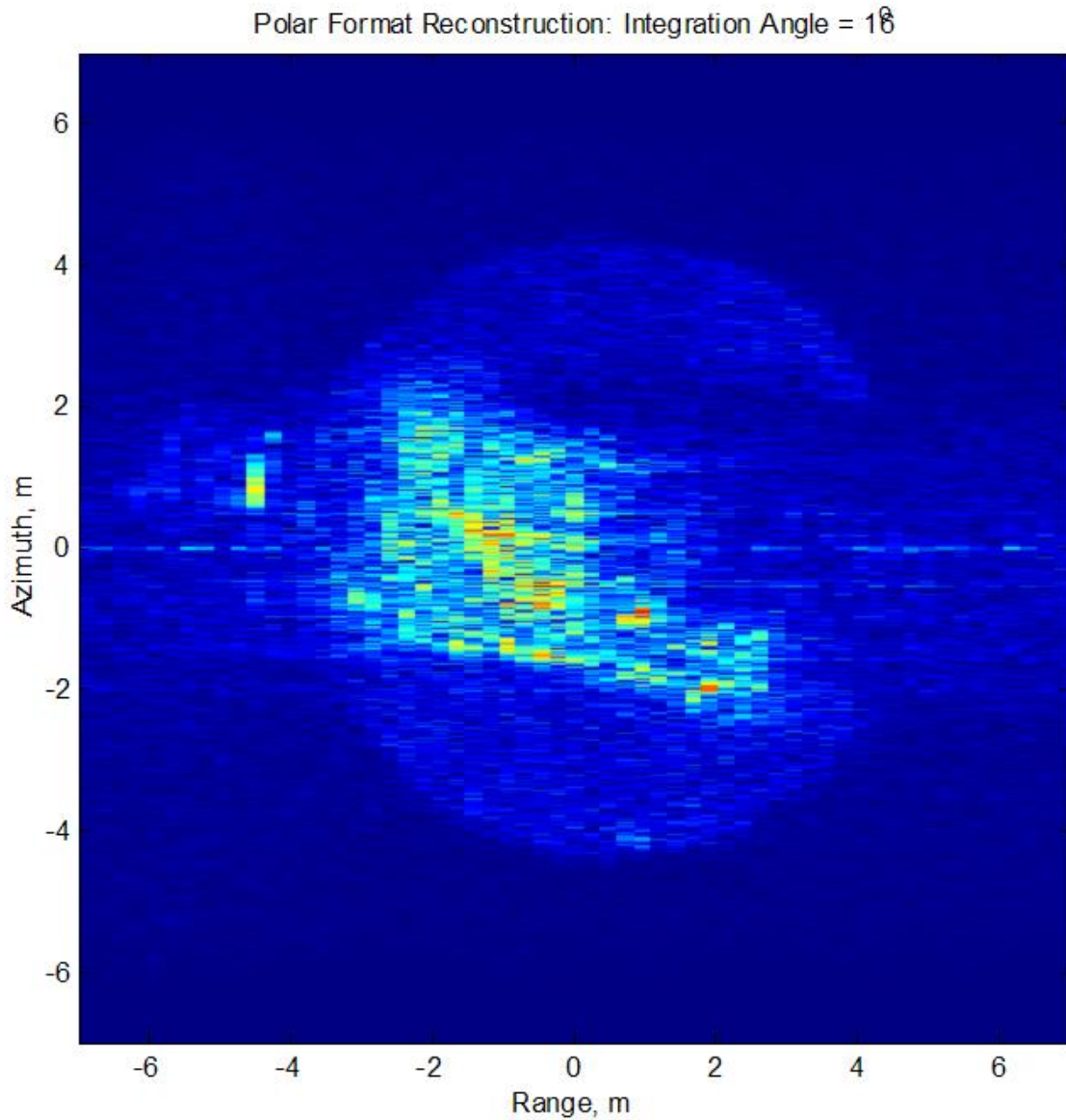
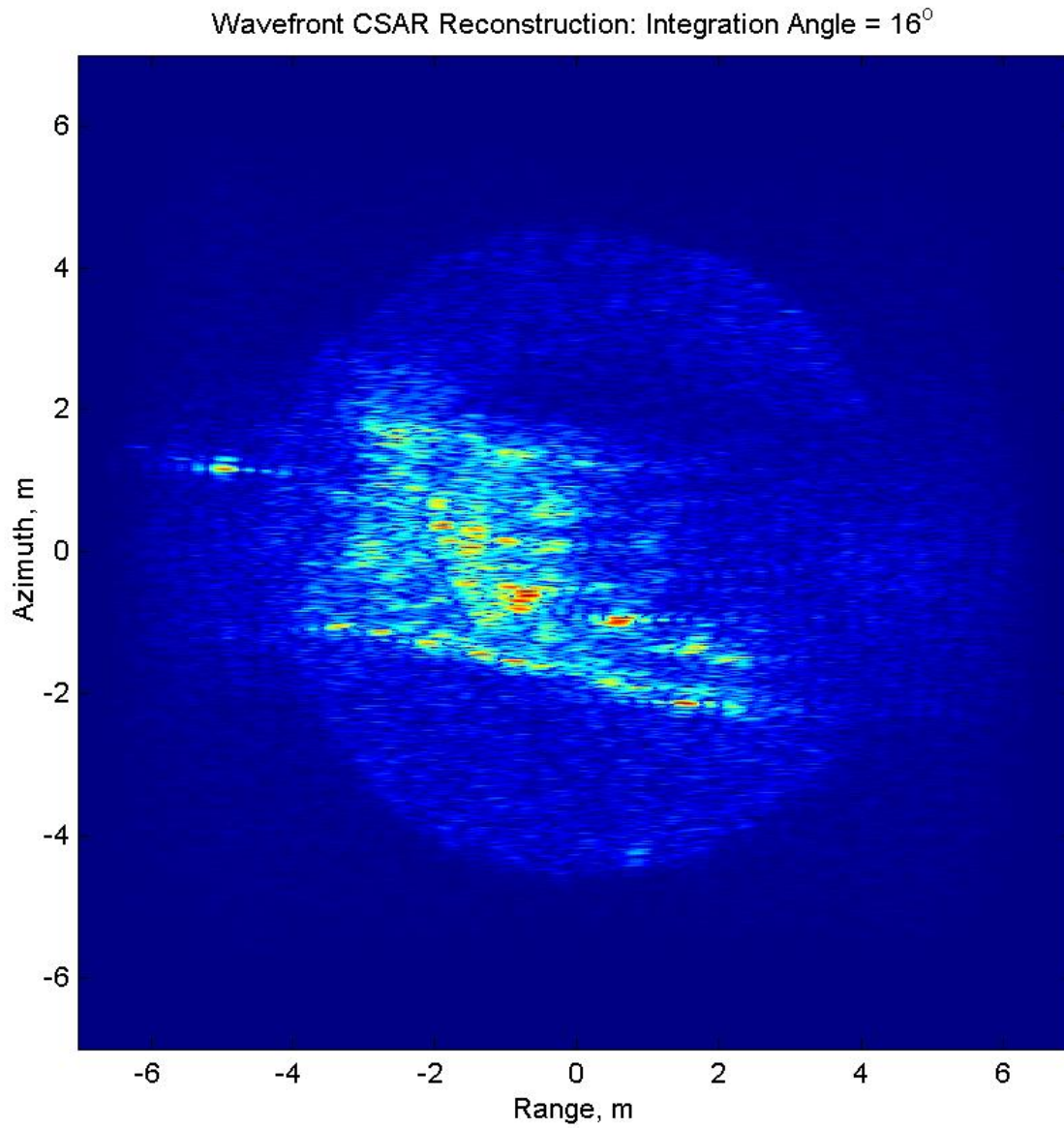


Figure 3c. Calibrated ISAR Data

A simple differencing or correlation of the two ISAR images would not indicate a match. Figures 6a and 6b, respectively, show the incoming and outgoing signal subspace difference (SSD) images. Note that the T-72 components are matched except for the gun and an area near the upper hatch. The latter might be an unintended change that occurred while moving the tank on and off the turntable. This can also be seen in Figure 7a and 7b that are the close ups of the original ISAR images and SSD images.



**Figure 4a. Polar Format Reconstruction:
Integration Angle = 16 Degrees**



**Figure 4b. Wavefront Reconstruction:
Integration Angle = 16 Degrees**

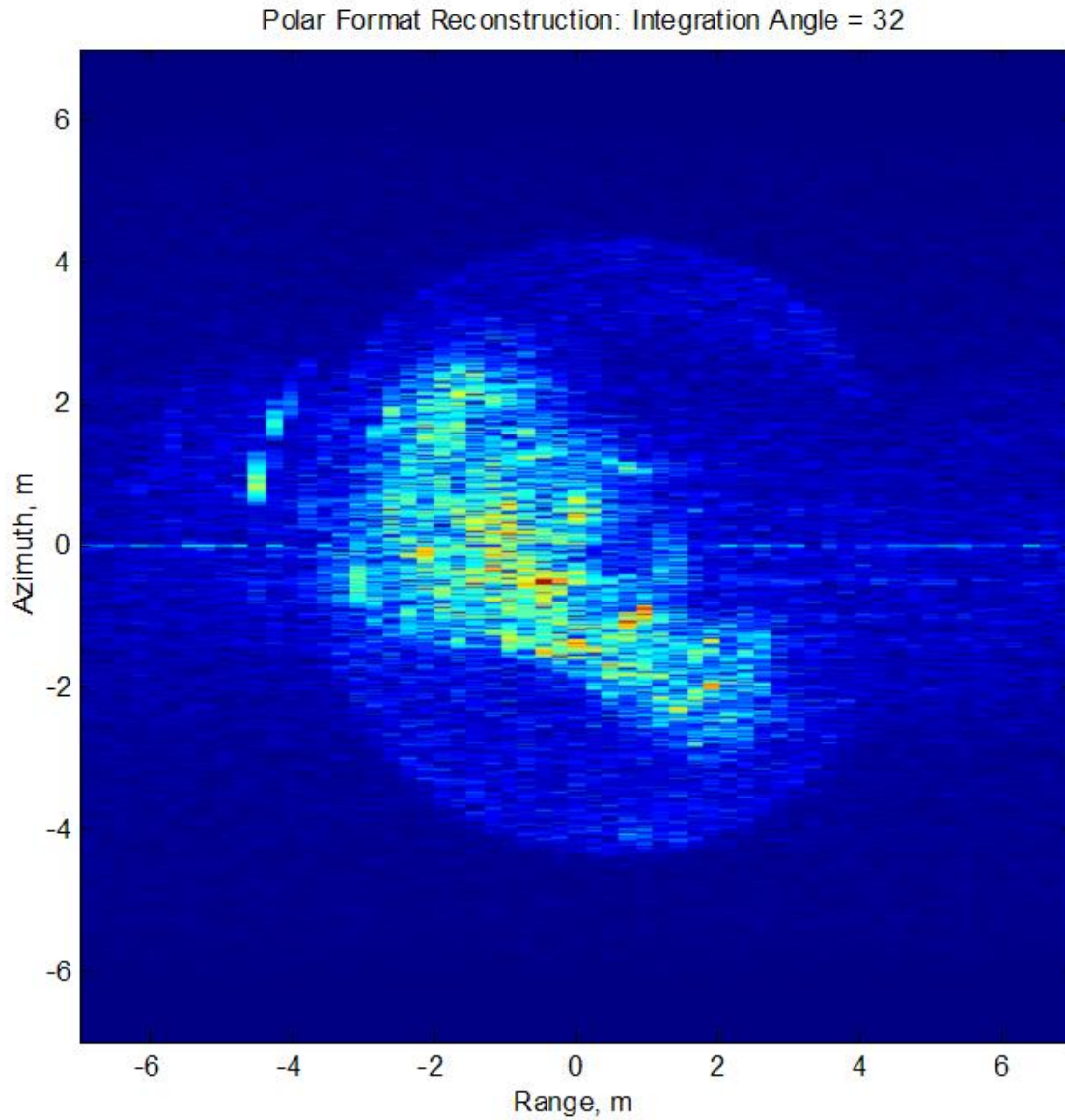


**Figure 5a. Polar Format Reconstruction:
Integration Angle = 32 Degrees**

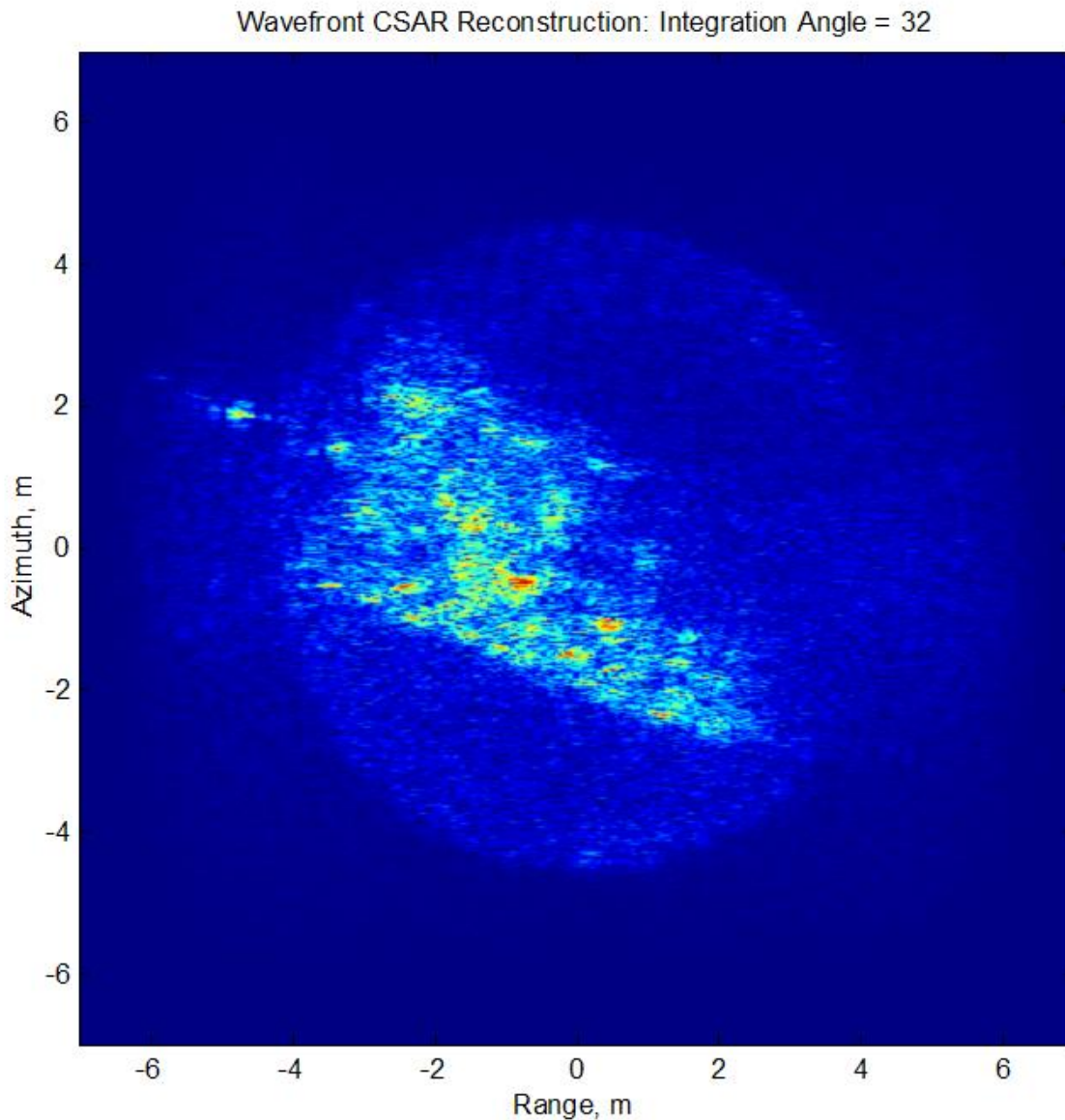


**Figure 5b. Wavefront Reconstruction:
Integration Angle = 32 Degrees**

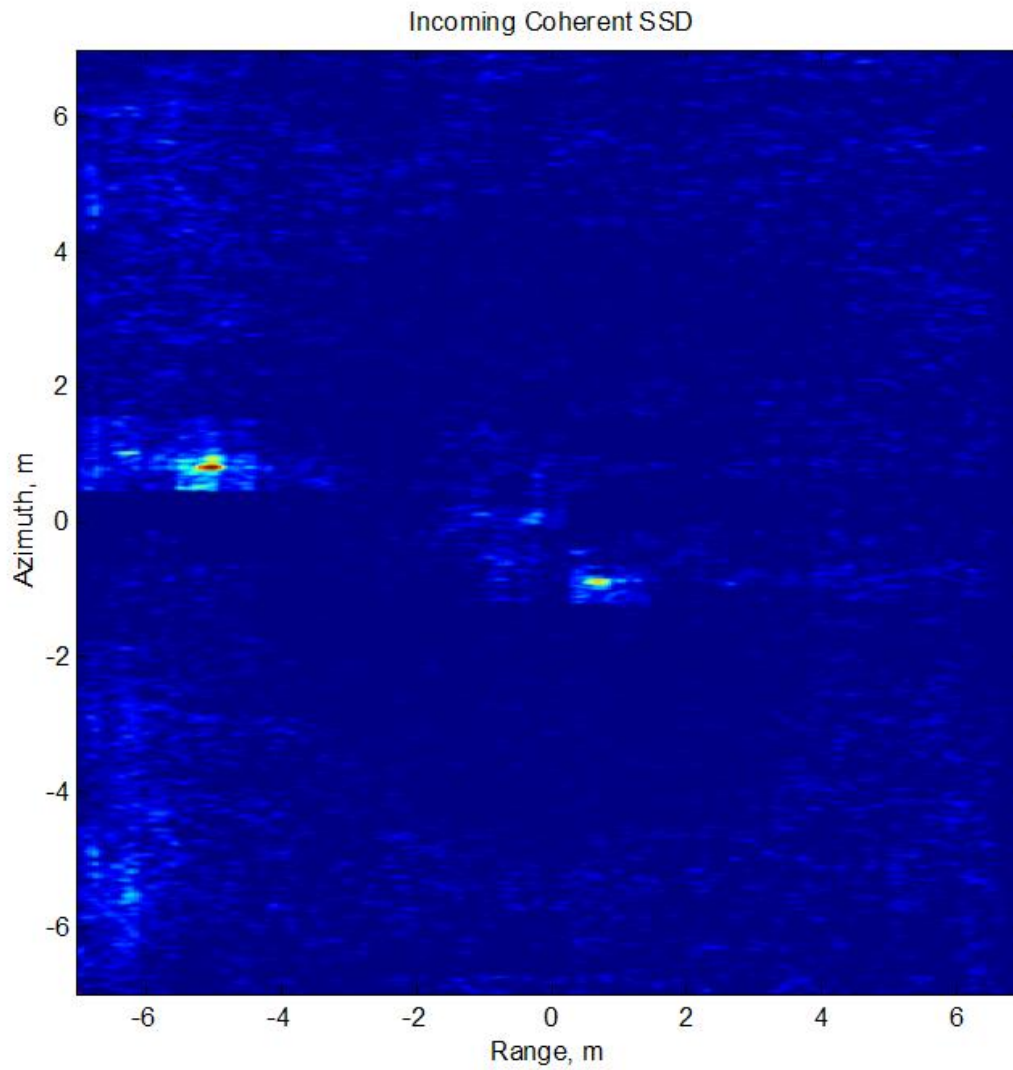


Figure 6a. Incoming Coherent Signal Subspace Difference

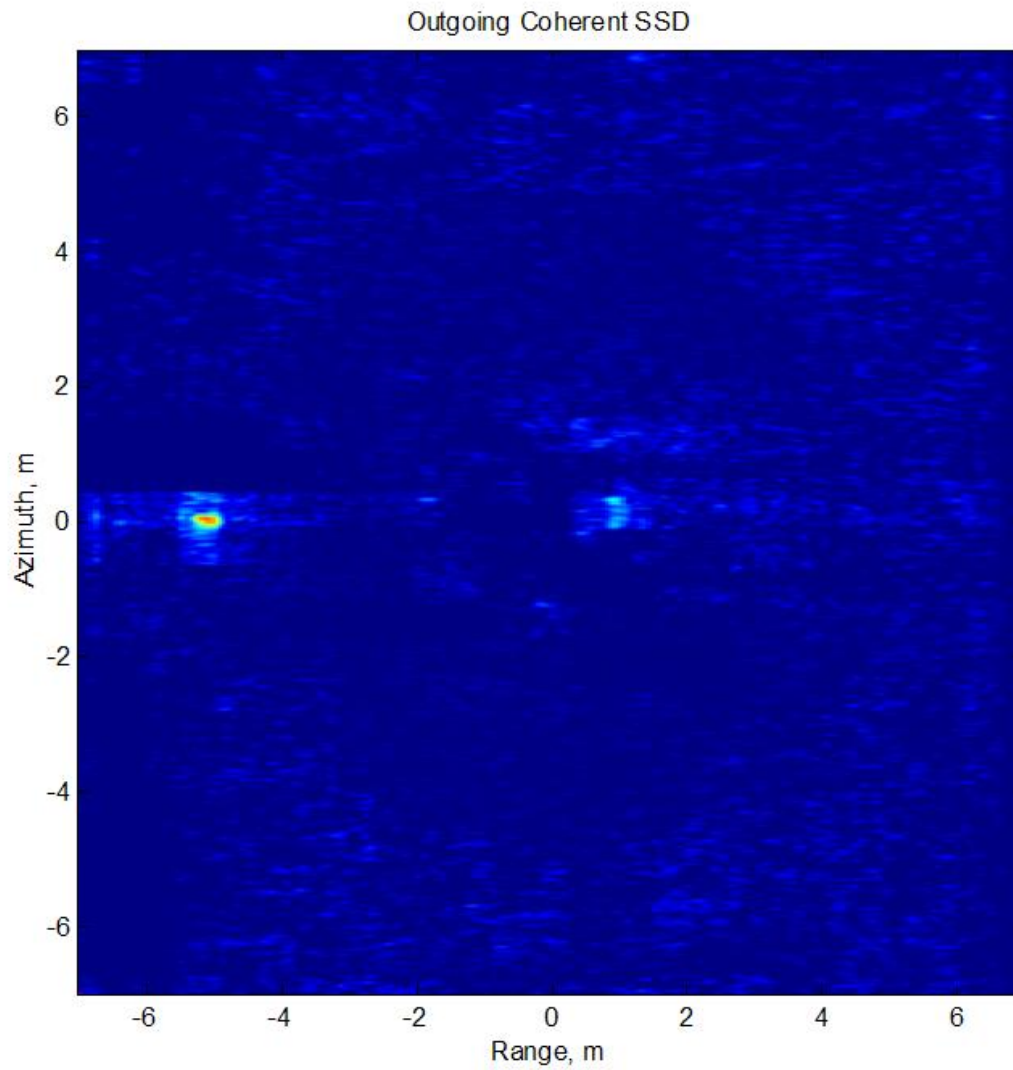


Figure 6b. Outgoing Coherent Signal Subspace Difference

Adaptive Processing of SAR Data for ATR

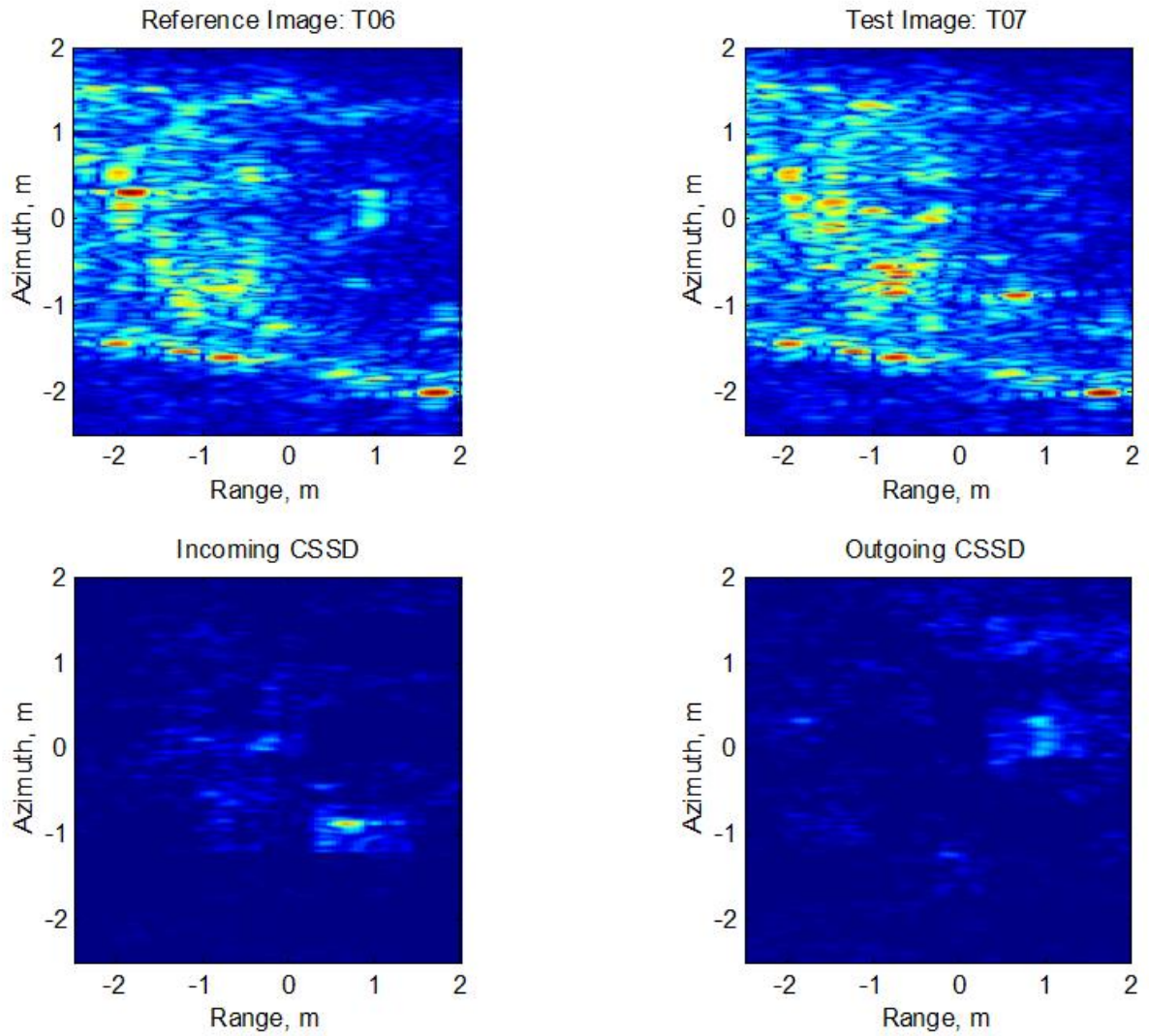


Figure 7a

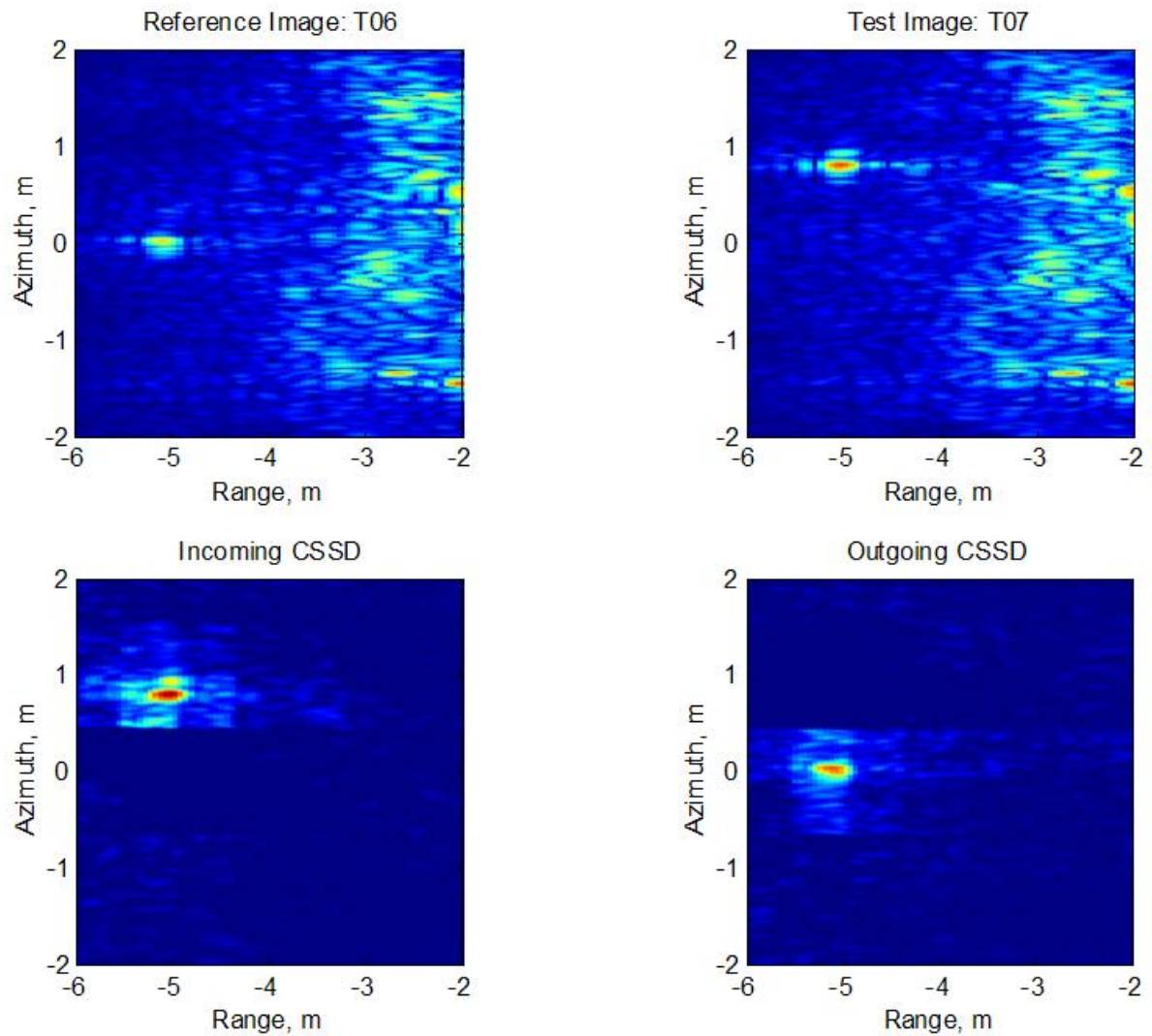


Figure 7b

5. Summary

Sensor calibration is a critical problem that has to be dealt with (though ignored) in noncoherent and coherent imaging systems such as SAR. Simple modification and/or reformulation of existing 1D adaptive (blind) filtering methods exist for 2D calibration problems of SAR-ATR, SAR-Coherent Change Detection (CCD), SAR-MTI, etc. This paper exhibited an example of the application this method in the SAR-ATR problem.

6. References

1. Soumekh, *SAR Signal Processing*, Wiley, 1999
2. Dilsavor, Mitra, Hensel, Soumekh, "GPS-Based Spatial and Spectral Registration of Delta-Heading Multipass SAR Imagery for Coherent Change Detection," *Proc. U.S. Army Workshop on Synthetic Aperture Radar Technology*, Redstone Arsenal, October 2002
3. Soumekh, "Moving Target Detection and Imaging Using an X Band Along-Track Monopulse SAR," *IEEE Trans. On Aerospace and Electronic Systems*, January 2002
4. Soumekh, Himed, "SAR-MTI Processing of Mutli-Channel Airborne Radar Measurement (MCARM) Data," *Proc. IEEE Radar Conf.*, May 2002

Adaptive Processing of SAR Data for ATR

Mehrdad Soumekh

M. Soumekh Consultant &
Department of Electrical Engineering
332 Bonner Hall, SUNY-Buffalo
Amherst, NY 14260
Phone: (716) 645-3115 x 2138
Email: msoum@eng.buffalo.edu

Outline

- Sources of Calibration Errors in SAR
 - Radar Calibration Errors
 - Target Signature Variations
- Model for Generation of SAR Signal
- Adaptive Calibration of Dual SAR Imagery via Signal Subspace Processing (SSP)
- Example: Ka Band Turntable (ISAR) Data
- Summary

Sources of Calibration Errors in SAR

Sources of Calibration Errors

- SAR signature of a target depends on the radar sensor characteristics (beam pattern, signal generator, etc.) as well as the physical properties of the target
- In SAR-ATR, comparison between the test and reference target chips requires understanding and incorporating the sensor and platform variations in the corresponding SAR data acquisitions

Sources of Calibration Errors, Cont.

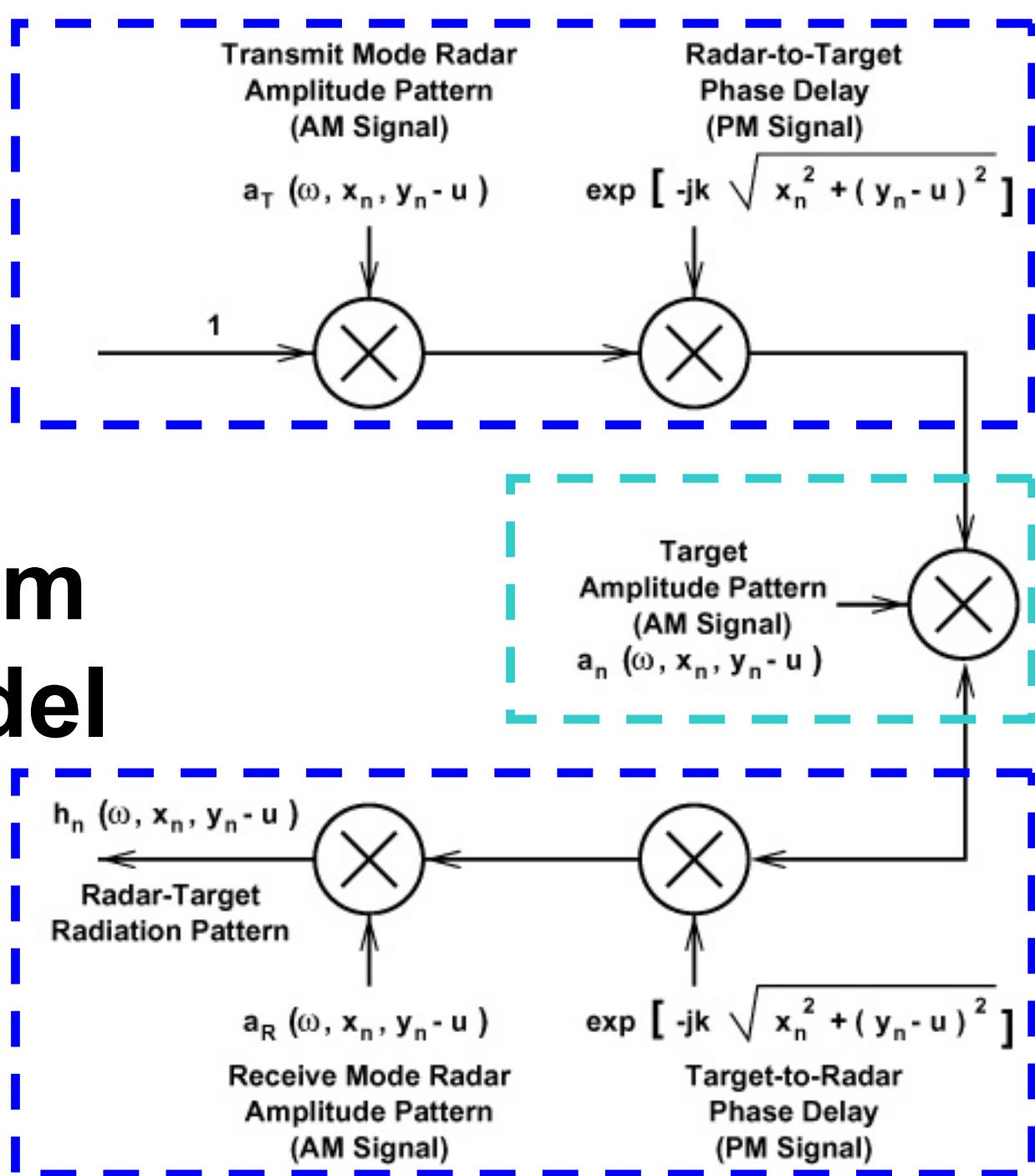
- The sensor variations are caused by various subtle changes (imperfections) in the radar system circuitry (e.g., waveform generator, cables, etc.), and undesirable amplitude/phase fluctuations in the radiation pattern of the physical radar between the reference and test data collections
- These are unknown and result in different 2D *Image Point Response* (IPR) or *Point Spread Function* (PSF) in the reference and test SAR images

Sources of Calibration Errors, Cont.

- These ambiguities result in unknown subtle geometric distortions and complex PSF variations in the reconstructed SAR image that have adverse effects on the performance of any SAR-ATR algorithm
- Variations in the target may also exist; e.g., rotation in the gun of a tank, opening or closing of driver/commander/turret hatch, etc.

Model for Generation of SAR Signal

Overall SAR System Signal Model



Variations in Radar Transmit-Mode Beam Pattern

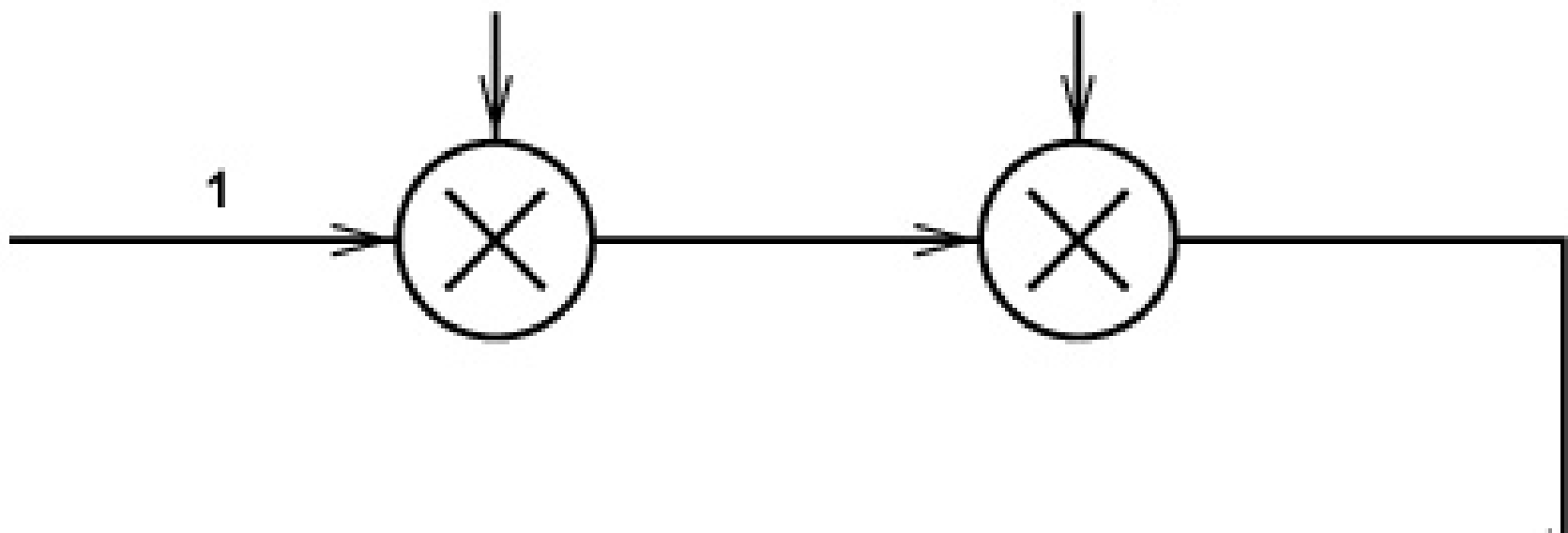
Variations in Motion & Autofocus

Transmit Mode Radar
Amplitude Pattern
(AM Signal)

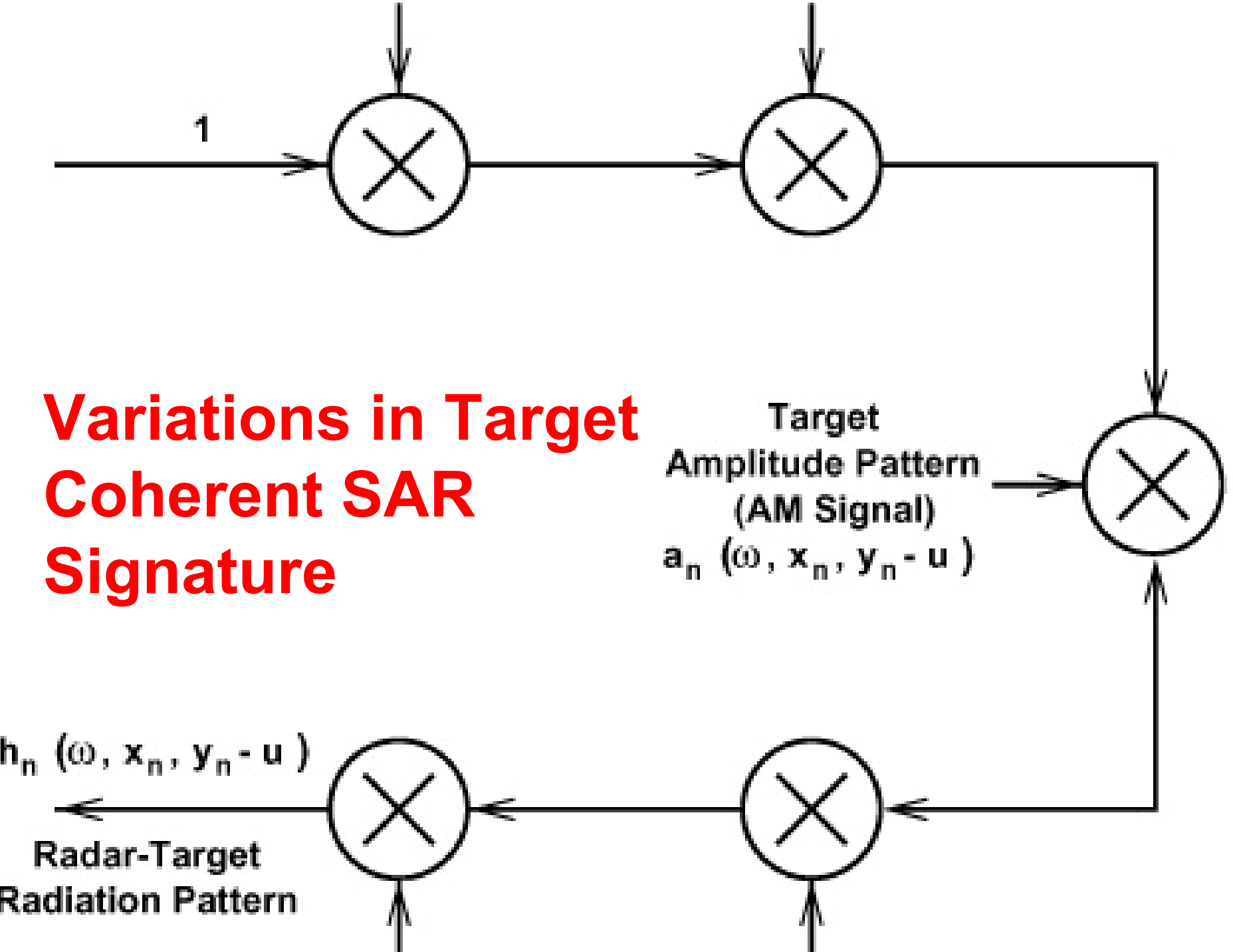
$$a_T(\omega, x_n, y_n - u)$$

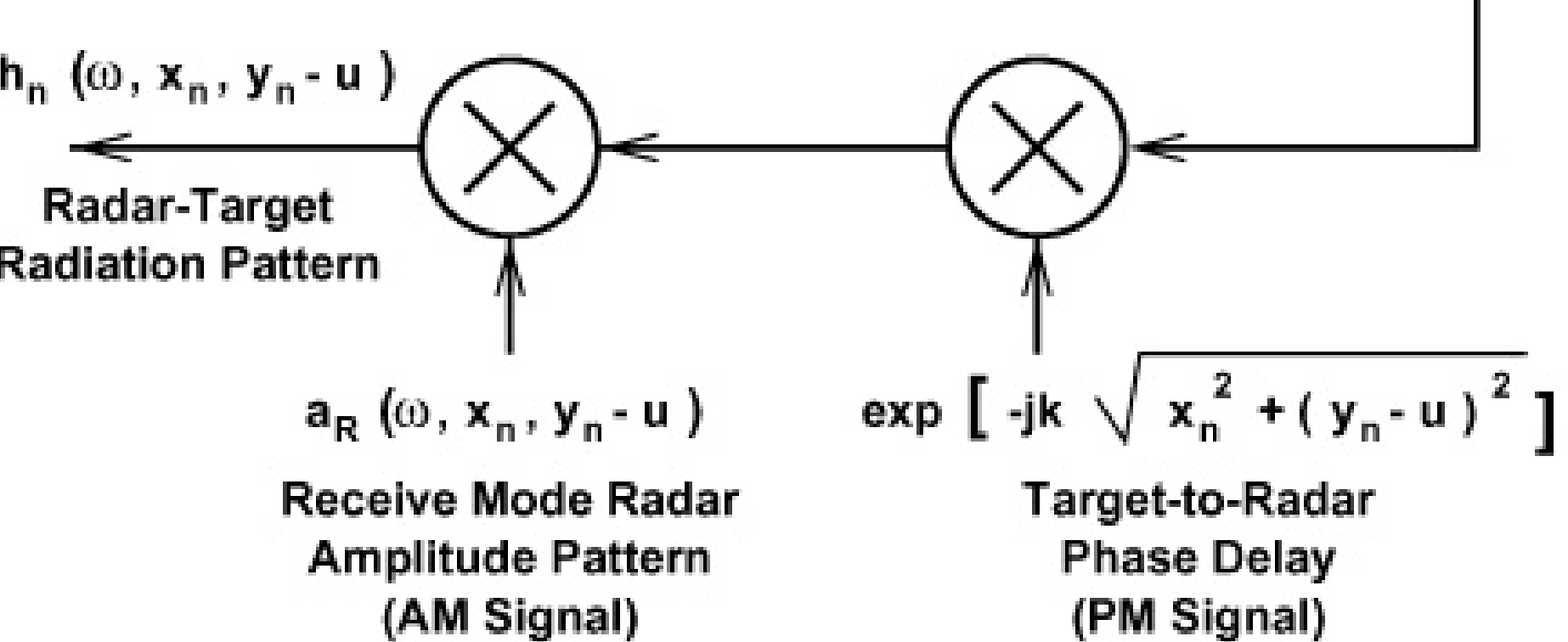
Radar-to-Target
Phase Delay
(PM Signal)

$$\exp \left[-jk \sqrt{x_n^2 + (y_n - u)^2} \right]$$



Variations in Target Coherent SAR Signature





Variations in Radar Receive-Mode Beam Pattern

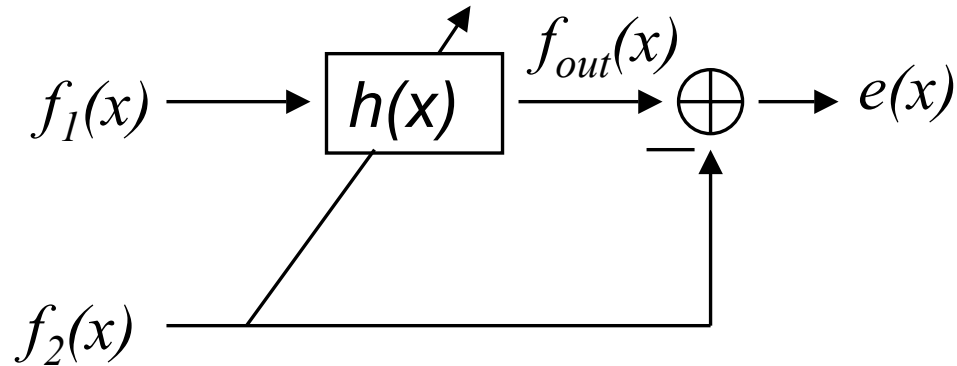
Variations in Motion & Autofocus

Adaptive Calibration of Dual SAR Imagery via Signal Subspace Processing

Adaptive SAR-ATR Solution

- A 2D *adaptive* method for the matching of test and reference target chips is utilized
- This algorithm, that we call *signal subspace matched filtering*, is not sensitive to the calibration errors of the SAR system (i.e., variations of the radar radiation pattern, etc. from one experiment to another) as well as small variations in the target

Signal Subspace Processing: A 1D Example



We want to determine $h(x)$ such that $f_1(x) = f_2(x)$ (i.e. $e(x) = 0$), for the example this means that we must determine $h(i)$ for $i = -2, \dots, 2$. The equations for the output of $h(x)$ are:

$$\begin{array}{rcccccc}
 f_1(-2)h(-2) + & f_1(-1)h(-1) + & f_1(0)h(0) + & f_1(1)h(1) + & f_1(2)h(2) = & f_{out}(0) \\
 f_1(-1)h(-2) + & f_1(0)h(-1) + & f_1(1)h(0) + & f_1(2)h(1) + & f_1(3)h(2) = & f_{out}(1) \\
 f_1(0)h(-2) + & f_1(1)h(-1) + & f_1(2)h(0) + & f_1(3)h(1) + & f_1(4)h(2) = & f_{out}(2) \\
 \vdots & & \vdots & & \vdots & \vdots \\
 f_1(n-2)h(-2) + & f_1(n-1)h(-1) + & f_1(n)h(0) + & f_1(n+1)h(1) + & f_1(n+2)h(2) = & f_{out}(n)
 \end{array}$$

This can be represented in vector form as shown on the next slide....

Signal Subspace Processing: A 1D Example, Cont.

$$\begin{array}{cccccc}
 \begin{bmatrix} f_1(-2) \\ f_1(-1) \\ \vdots \\ f_1(n-2) \end{bmatrix} & h(-2) + & \begin{bmatrix} f_1(-1) \\ f_1(0) \\ \vdots \\ f_1(n-1) \end{bmatrix} & h(-1) + & \begin{bmatrix} f_1(0) \\ f_1(1) \\ \vdots \\ f_1(n) \end{bmatrix} & h(0) + & \begin{bmatrix} f_1(1) \\ f_1(2) \\ \vdots \\ f_1(n+1) \end{bmatrix} & h(1) + & \begin{bmatrix} f_1(2) \\ f_1(3) \\ \vdots \\ f_1(n+2) \end{bmatrix} & h(2) = & \begin{bmatrix} f_{out}(0) \\ f_{out}(1) \\ \vdots \\ f_{out}(n) \end{bmatrix} \\
 \parallel & & \parallel \\
 \mathbf{V}_{-2} & & \mathbf{V}_{-1} & & \mathbf{V}_0 & & \mathbf{V}_1 & & \mathbf{V}_2 & & \mathbf{V}_{out}
 \end{array}$$

The vector representation shows that the output resides in the *signal subspace* spanned by $\mathbf{V} = \{\mathbf{v}_i, i = -2, \dots, 2\}$. We can create an orthonormal basis for this subspace (via Gram-Schmidt) and obtain modified filter coefficients based on these new basis vectors. That is:

$$\begin{aligned}
 & \mathbf{v}_{-2}h(-2) + \mathbf{v}_{-1}h(-1) + \mathbf{v}_0h(0) + \mathbf{v}_1h(1) + \mathbf{v}_2h(2) = \\
 & \hat{\mathbf{v}}_{-2}\hat{h}(-2) + \hat{\mathbf{v}}_{-1}\hat{h}(-1) + \hat{\mathbf{v}}_0\hat{h}(0) + \hat{\mathbf{v}}_1\hat{h}(1) + \hat{\mathbf{v}}_2\hat{h}(2)
 \end{aligned}$$

Where the notation $\hat{\mathbf{v}}_i$ indicates that the vector is part of the orthonormal basis and the notation $\hat{h}(i)$ indicates that the coefficient has been adjusted appropriately (for the orthonormal basis vector).

Signal Subspace Processing: A 1D Example, Cont.

We can solve for each of the filter coefficients by calculating the inner product with the corresponding orthonormal basis vector:

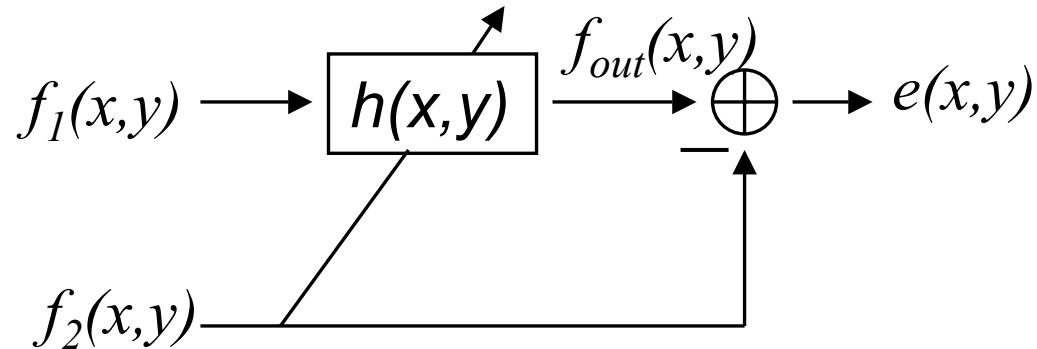
$$\begin{aligned}\hat{h}(i) &= \left\langle \hat{\mathbf{v}}_{-2}\hat{h}(-2) + \hat{\mathbf{v}}_{-1}\hat{h}(-1) + \hat{\mathbf{v}}_0\hat{h}(0) + \hat{\mathbf{v}}_1\hat{h}(1) + \hat{\mathbf{v}}_2\hat{h}(2), \hat{\mathbf{v}}_i \right\rangle \\ &= \left\langle \hat{\mathbf{v}}_i, \mathbf{v}_{out} \right\rangle\end{aligned}$$

These coefficients can then be used to calculate the projection of $f_2(x)$ signal into the signal subspace of $f_1(x)$.

→ The resulting output of $h(x)$ (the estimate of $f_2(x)$) is simply the projection of $f_2(x)$ into the signal subspace of $f_1(x)$!!

The difference between the reference signal and the projected test signal becomes: $e = \hat{f}_2 - f_1$
which also shows how much the test signal differs from the reference.

Extension to 2D



Linear Filter:

$$f_2^{(k)}(x_i, y_j) = \sum_{m=-n_x}^{n_x} \sum_{n=-n_y}^{n_y} h_{mn}^{(k)} f_1^{(k)}(x_i - m\Delta_x, y_j - n\Delta_y)$$

Signal Subspace:

$$\Phi_1^{(k)} = [f_1^{(k)}(x_i - m\Delta_x, y_j - n\Delta_y); m = -n_x, \dots, n_x, n = -n_y, \dots, n_y]$$

Extension to 2D, Cont.

The orthonormalized Signal Subspace:

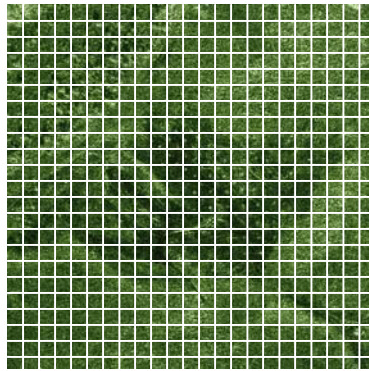
$$\Theta_1^{(k)} = \left[\theta_1^{(k)}(x_i - m\Delta_x, y_j - n\Delta_y); \quad m = -n_x, \dots, n_x, \quad n = -n_y, \dots, n_y \right. \\ \left. \begin{array}{l} x_i = x_{\min, k}, \quad x_{\min, k} + 1, \dots, x_{\max, k}, \\ y_j = y_{\min, k}, \quad y_{\min, k} + 1, \dots, y_{\max, k} \end{array} \right]$$

The filter output (for the normalized subspace):

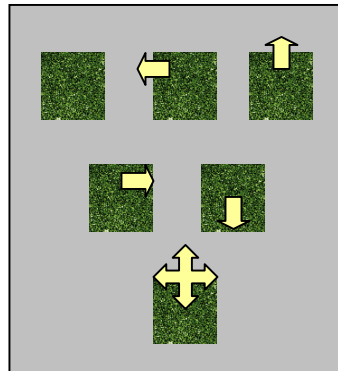
$$\hat{f}_2^{(k)}(x_i, y_j) = \sum_{m=-n_x}^{n_x} \sum_{n=-n_y}^{n_y} \hat{h}_{mn}^{(k)} f_1^{(k)}(x_i - m\Delta_x, y_j - n\Delta_y)$$

Analogous to the 1D case, the output of the filter is simply the projection of $f_2^{(k)}(x, y)$ into $\Theta^{(k)}$.

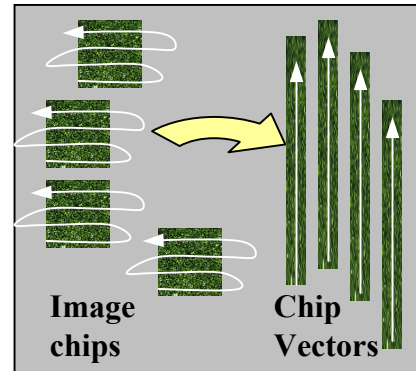
Signal Subspace Matching or Change Detection



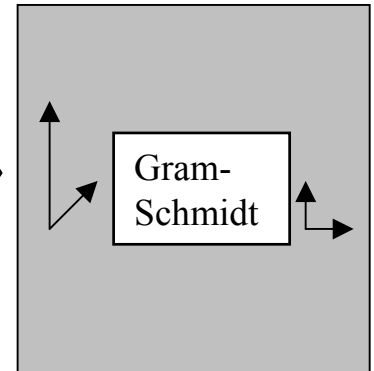
Create small, "local" image chips for both reference and test



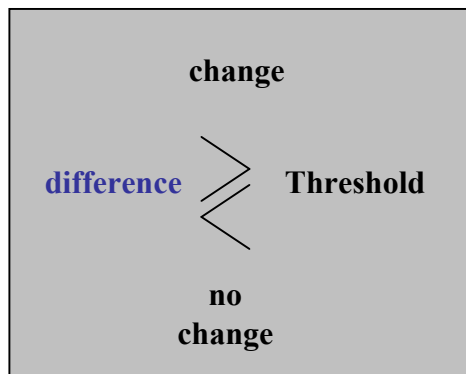
Shift each reference chip to create a "basis" for each grid square



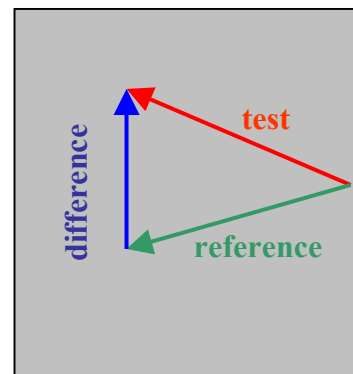
Create Reference Image Basis Vectors from Basis Chips



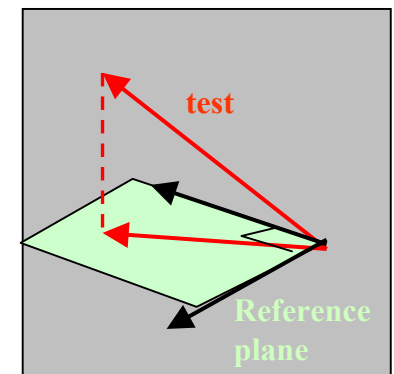
Orthonormalize Reference Image Basis Vectors



Decide if target has entered or exited scene



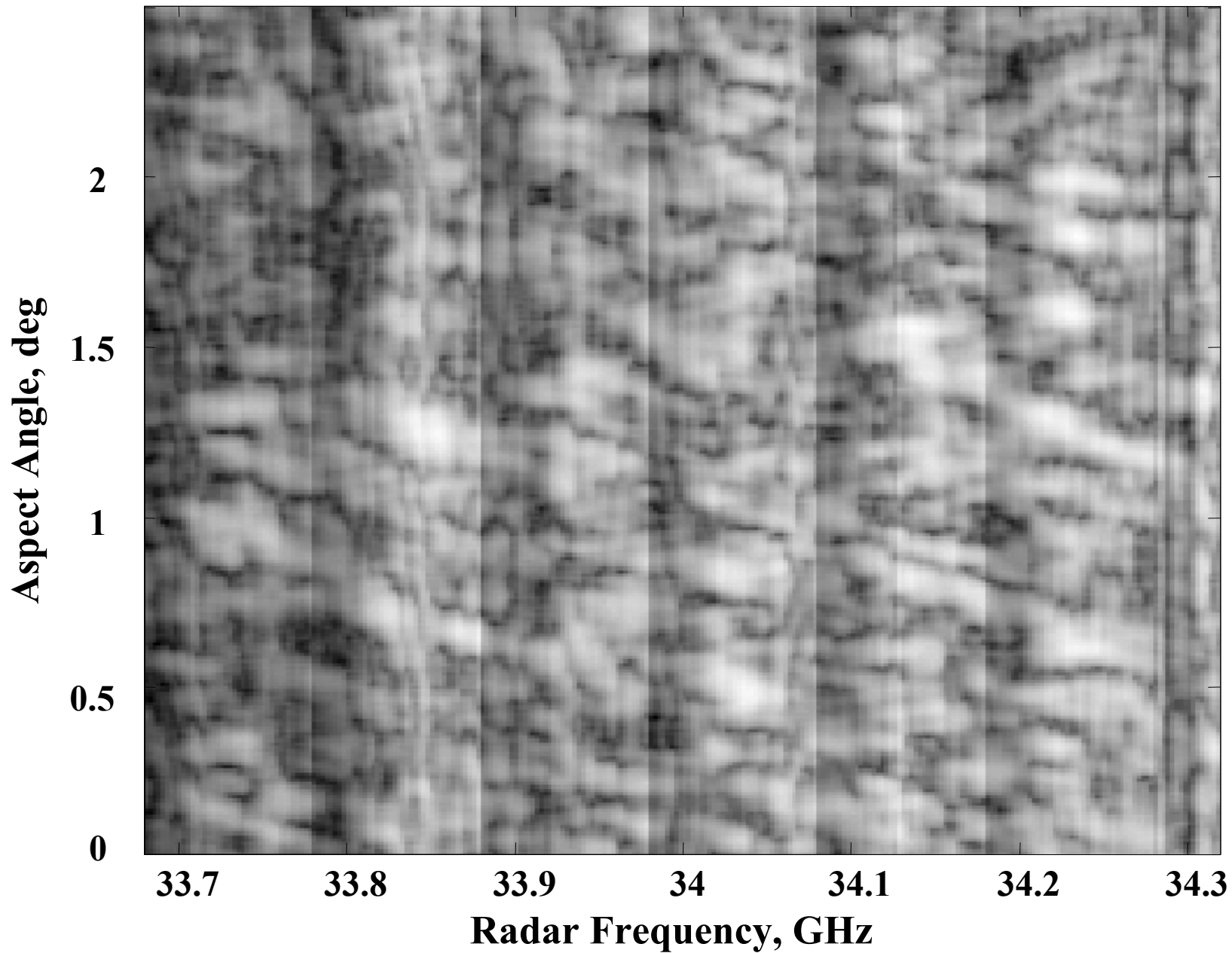
Subtract Reference from projection



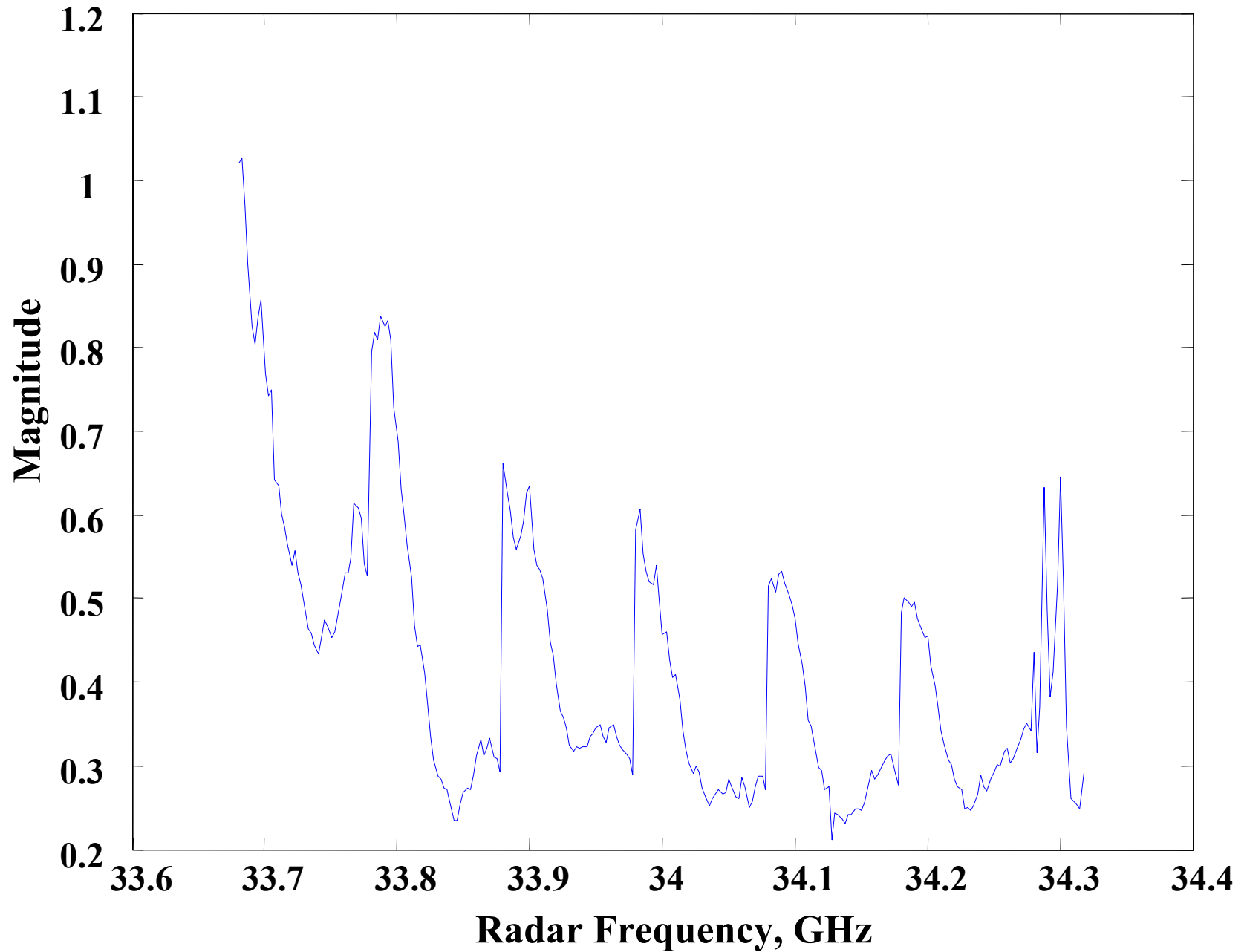
Project test vector into reference subspace

Adaptive SAR-ATR: Ka Band Turntable (ISAR) Data

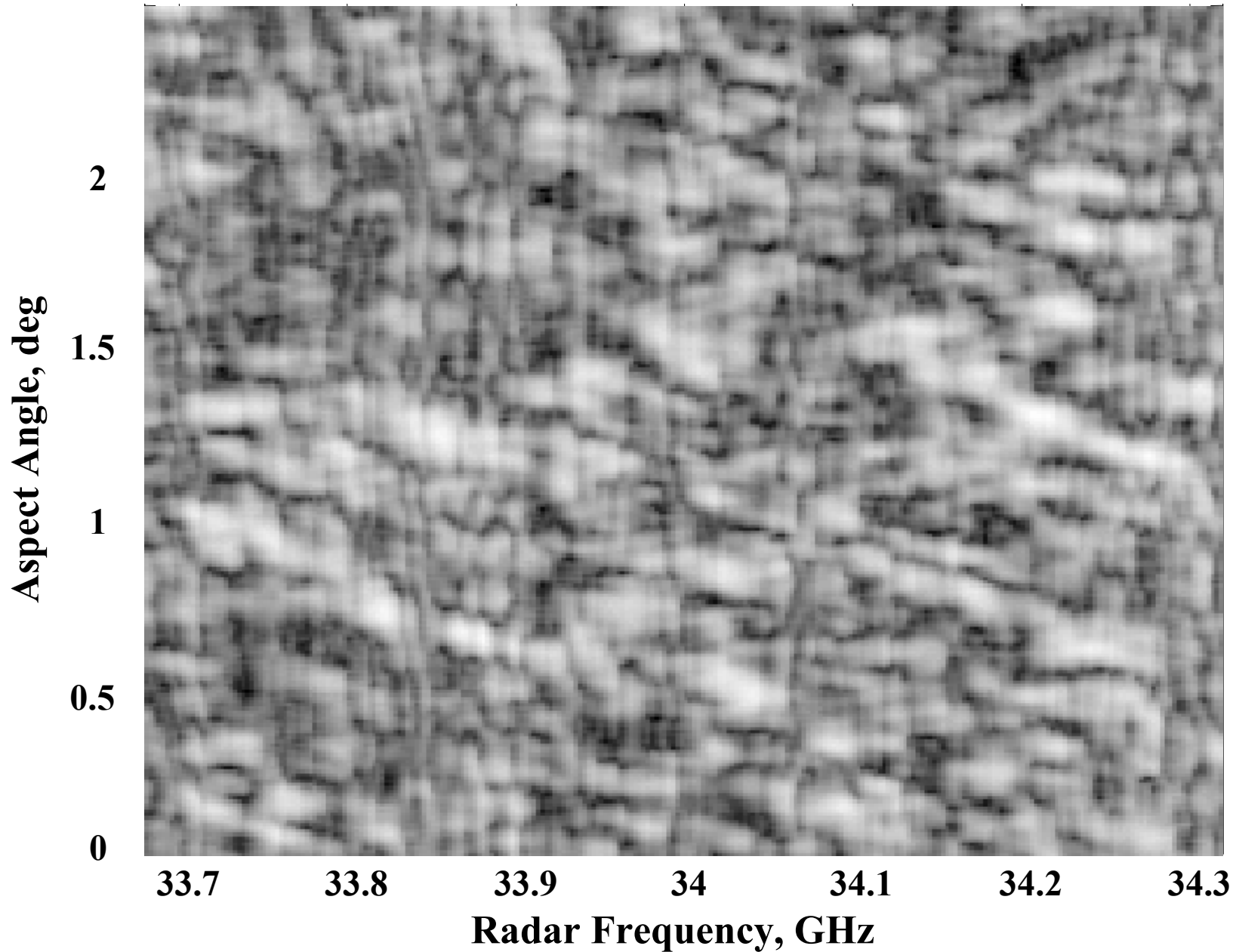
Measured SAR Data



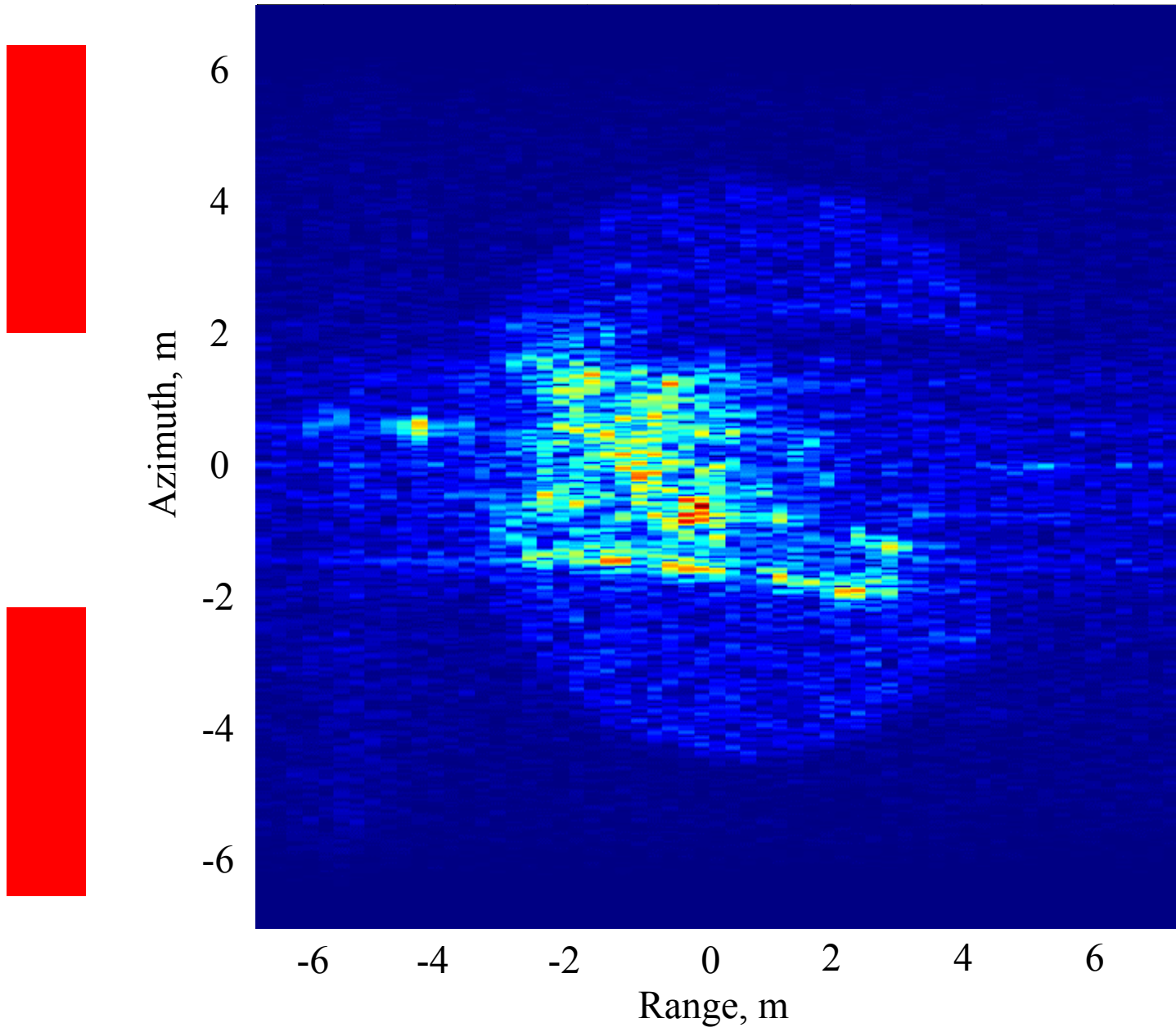
Cumulative Relative Magnitude



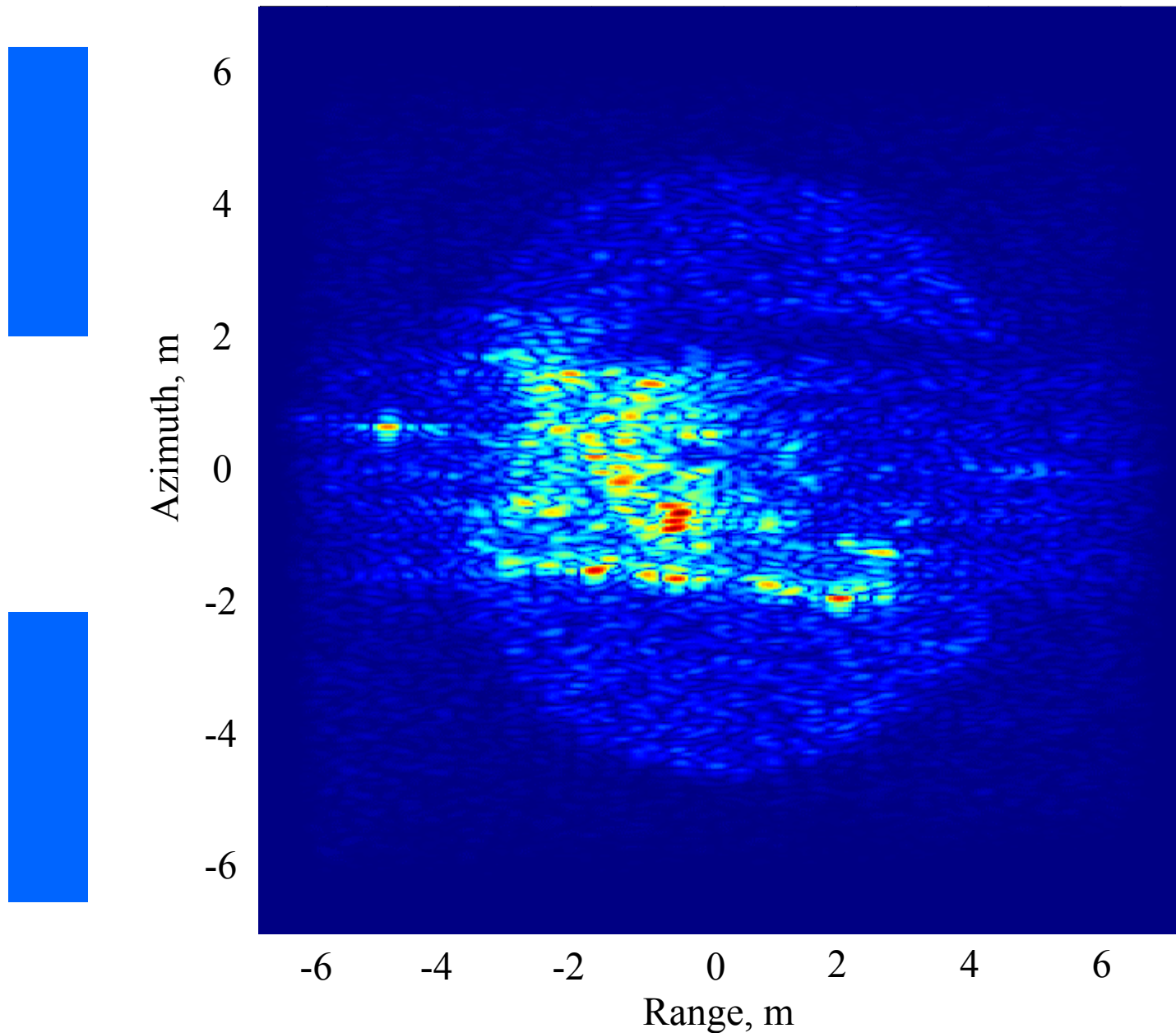
Magnitude Calibrated SAR Data



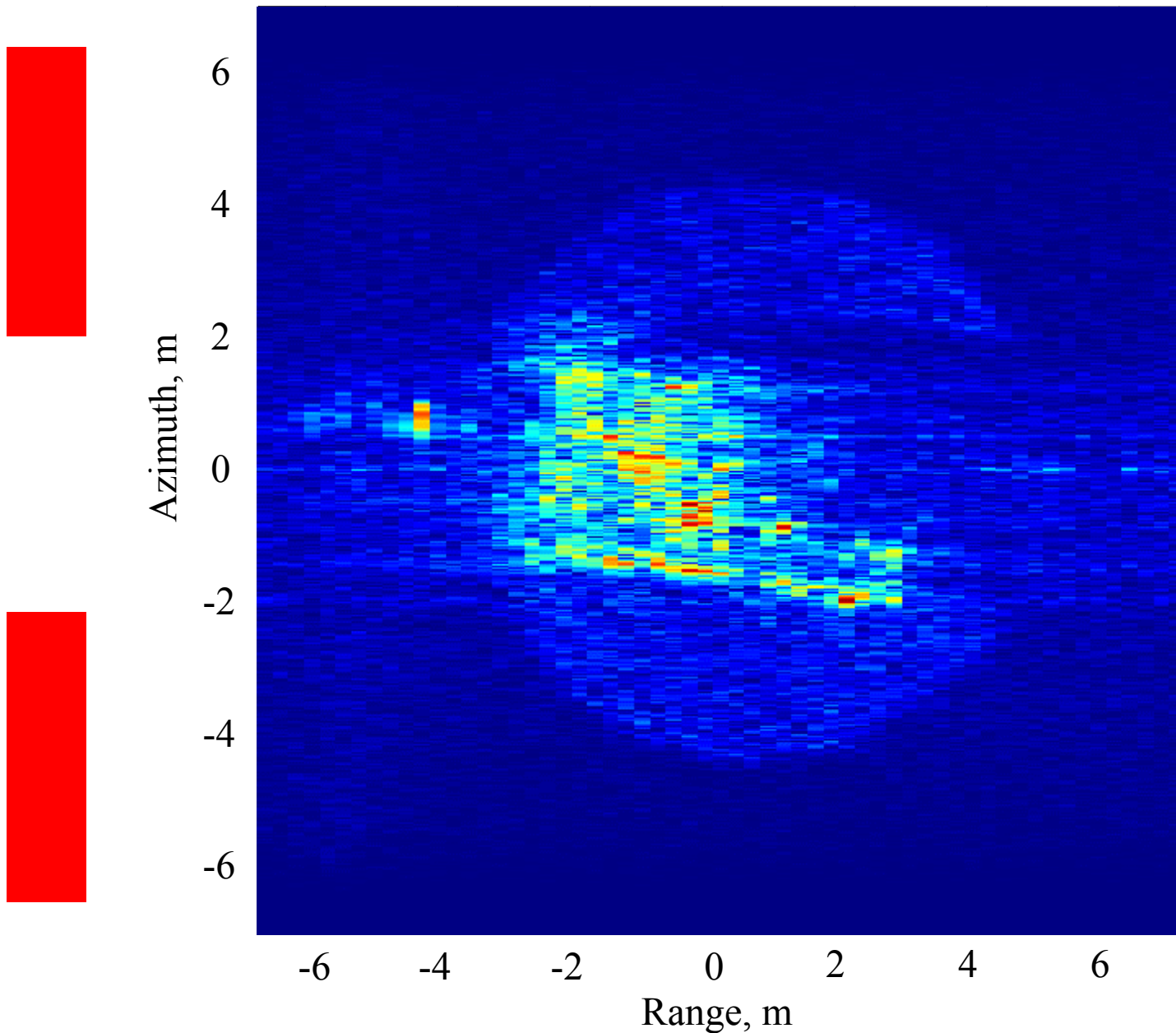
Polar Format Reconstruction: Integration Angle = 4



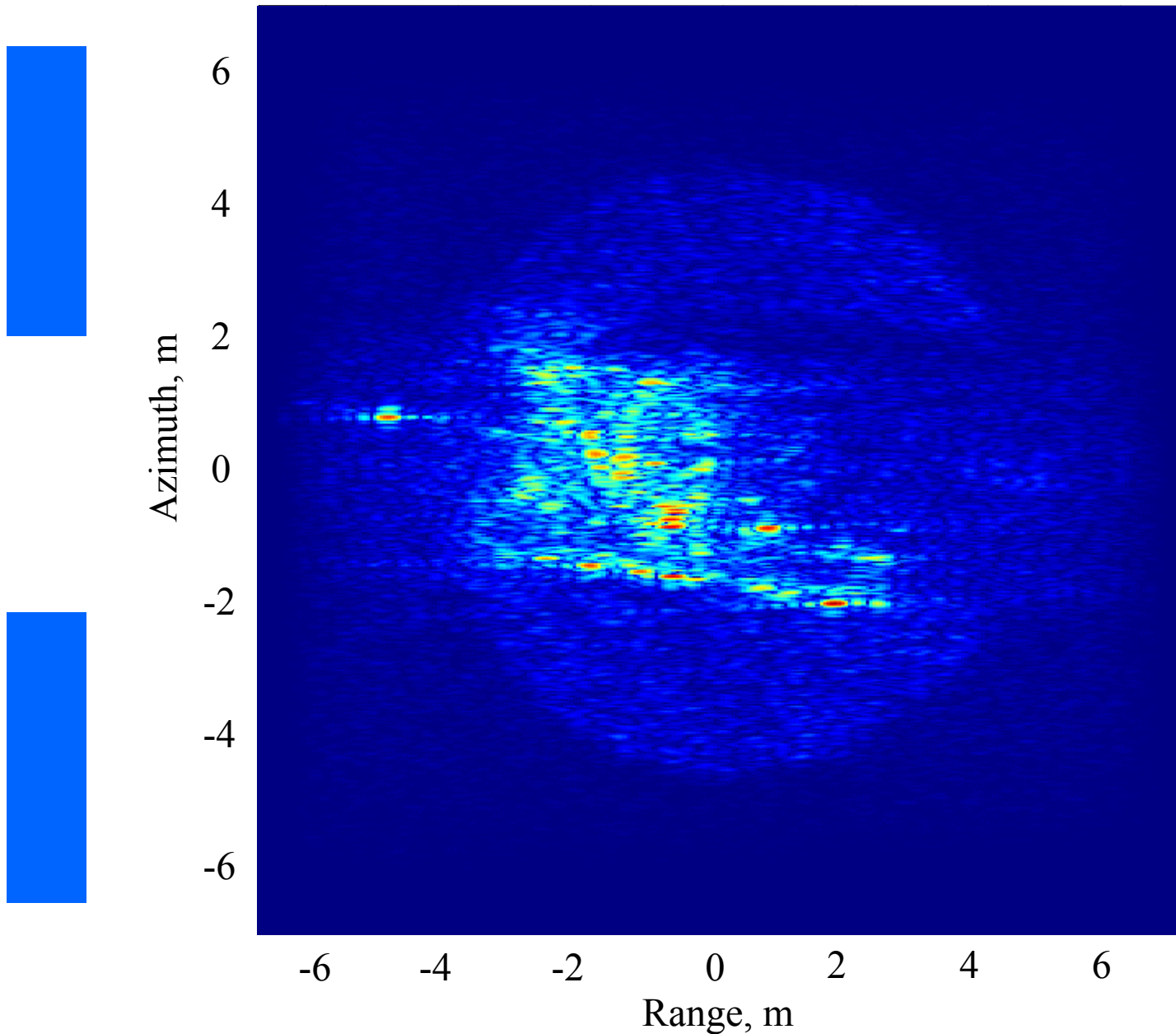
Wavefront CSAR Reconstruction: Integration Angle = 4



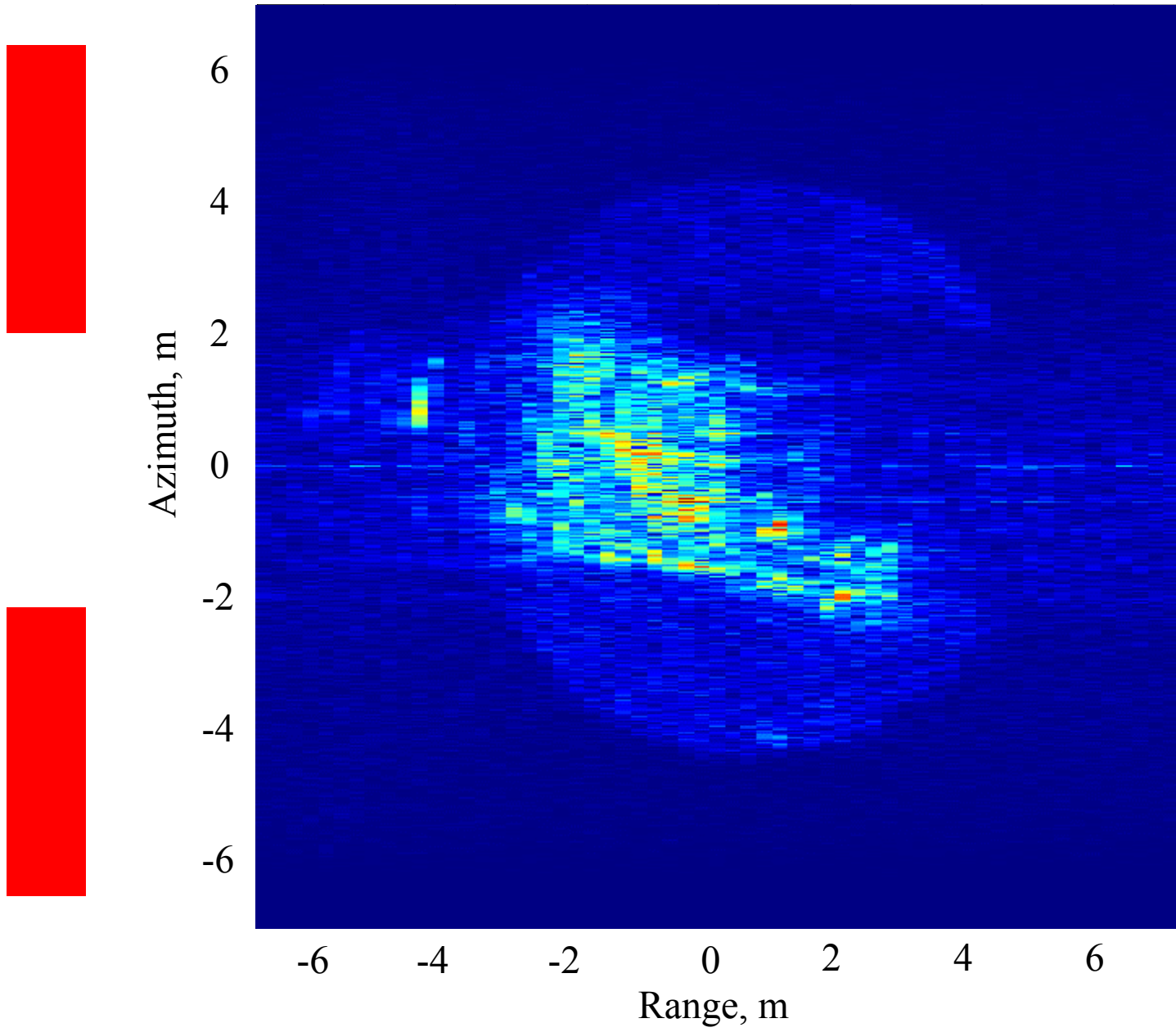
Polar Format Reconstruction: Integration Angle = 8



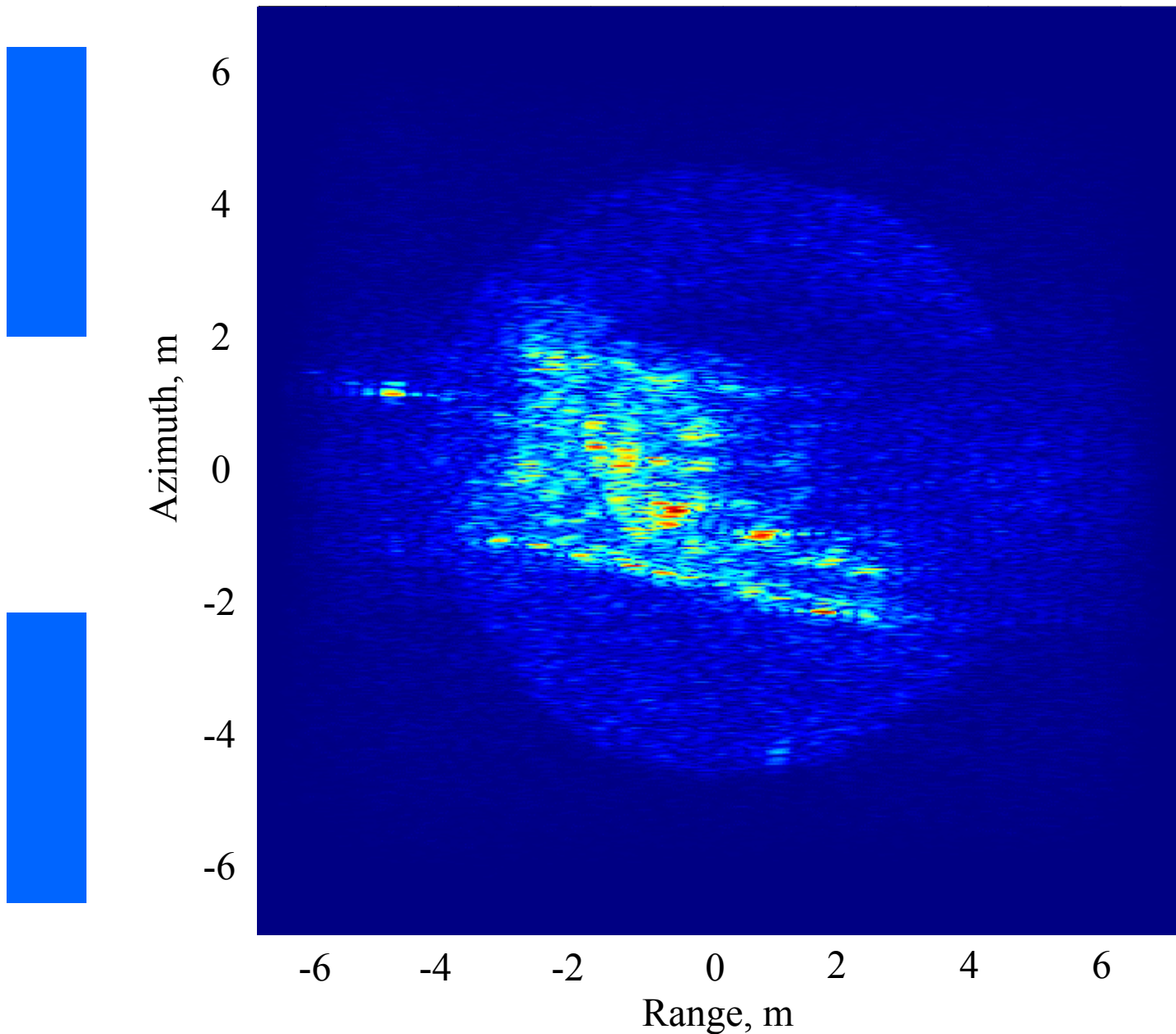
Wavefront CSAR Reconstruction: Integration Angle = 8



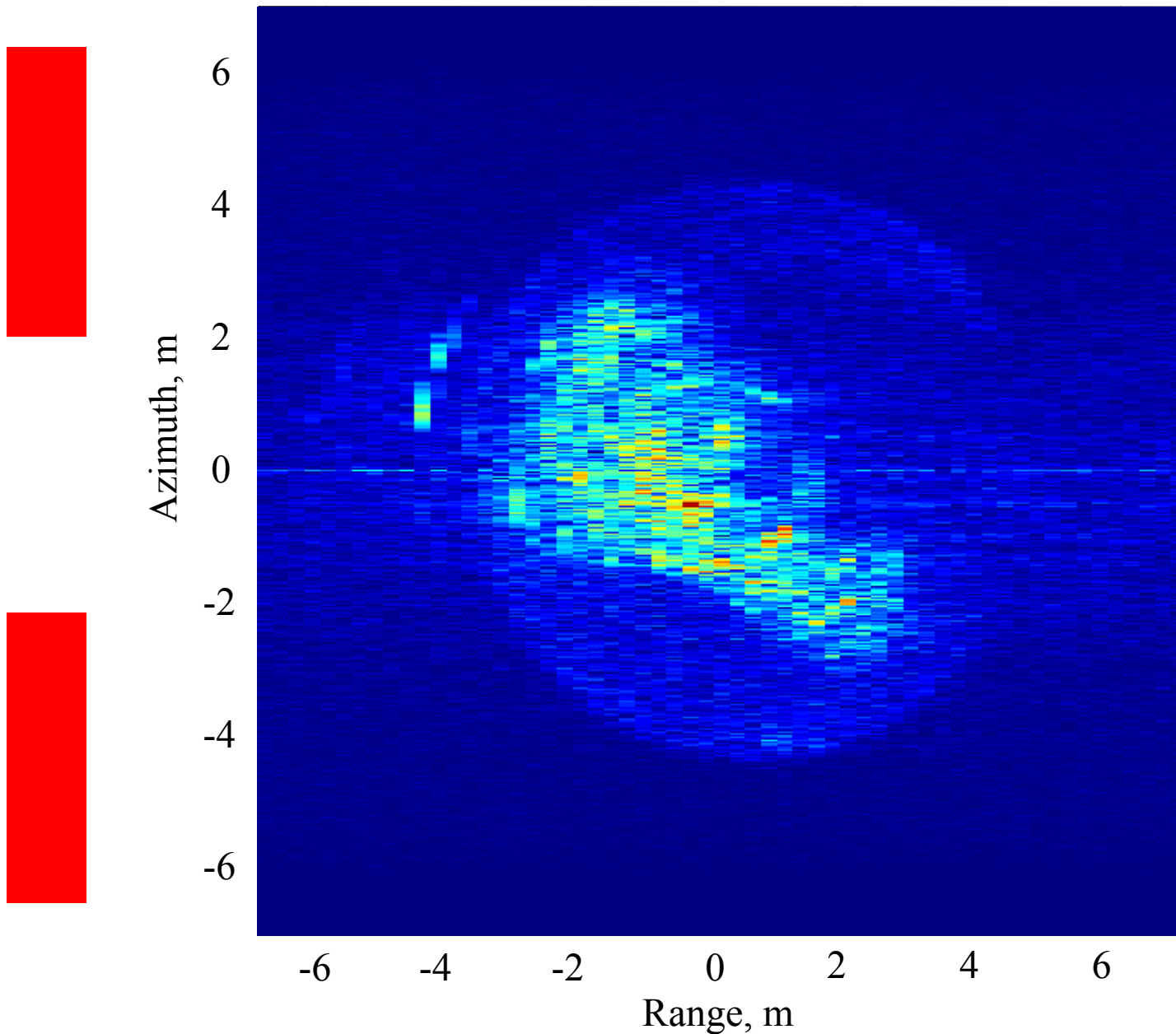
Polar Format Reconstruction: Integration Angle = 16



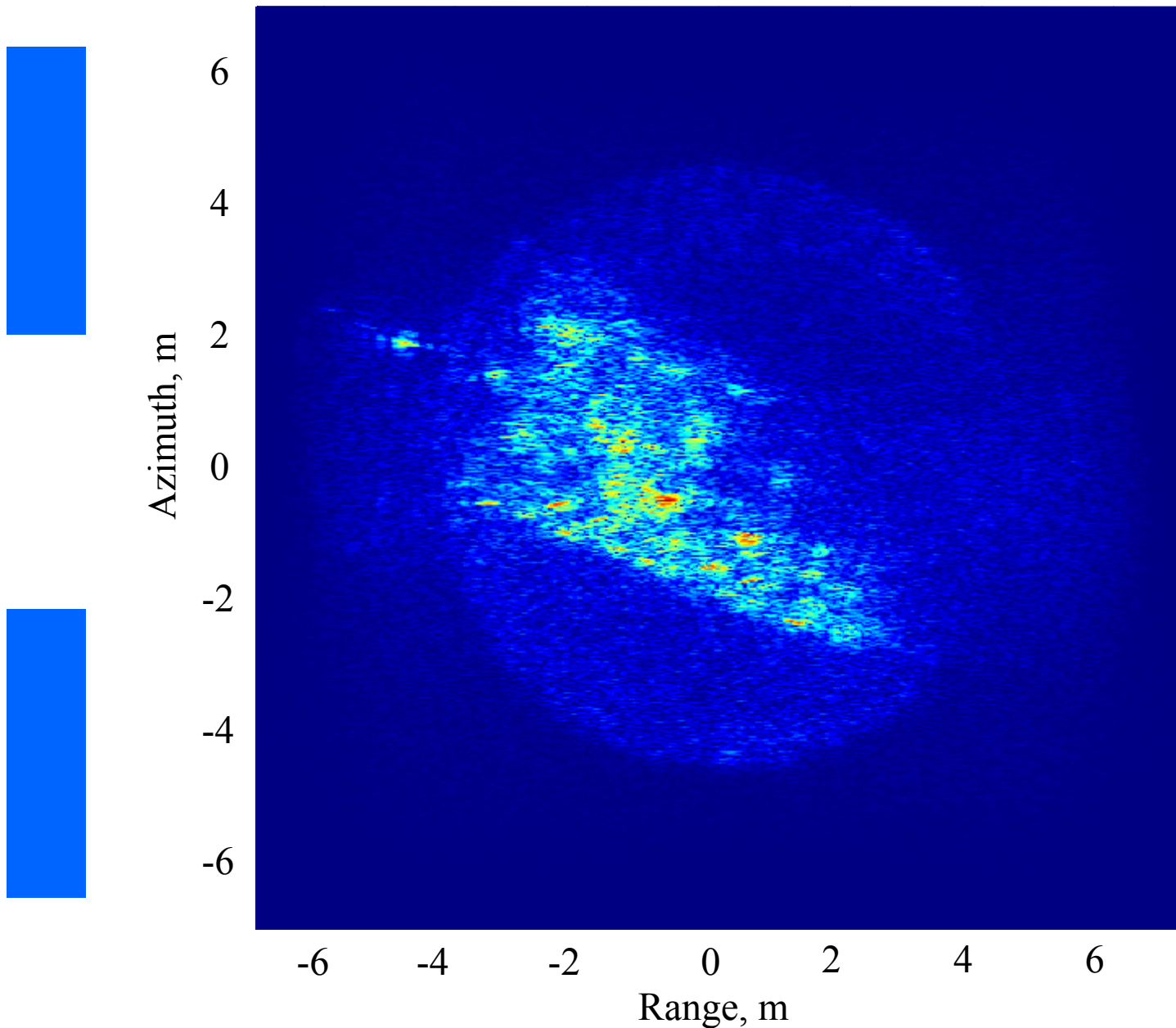
Wavefront CSAR Reconstruction: Integration Angle = 16



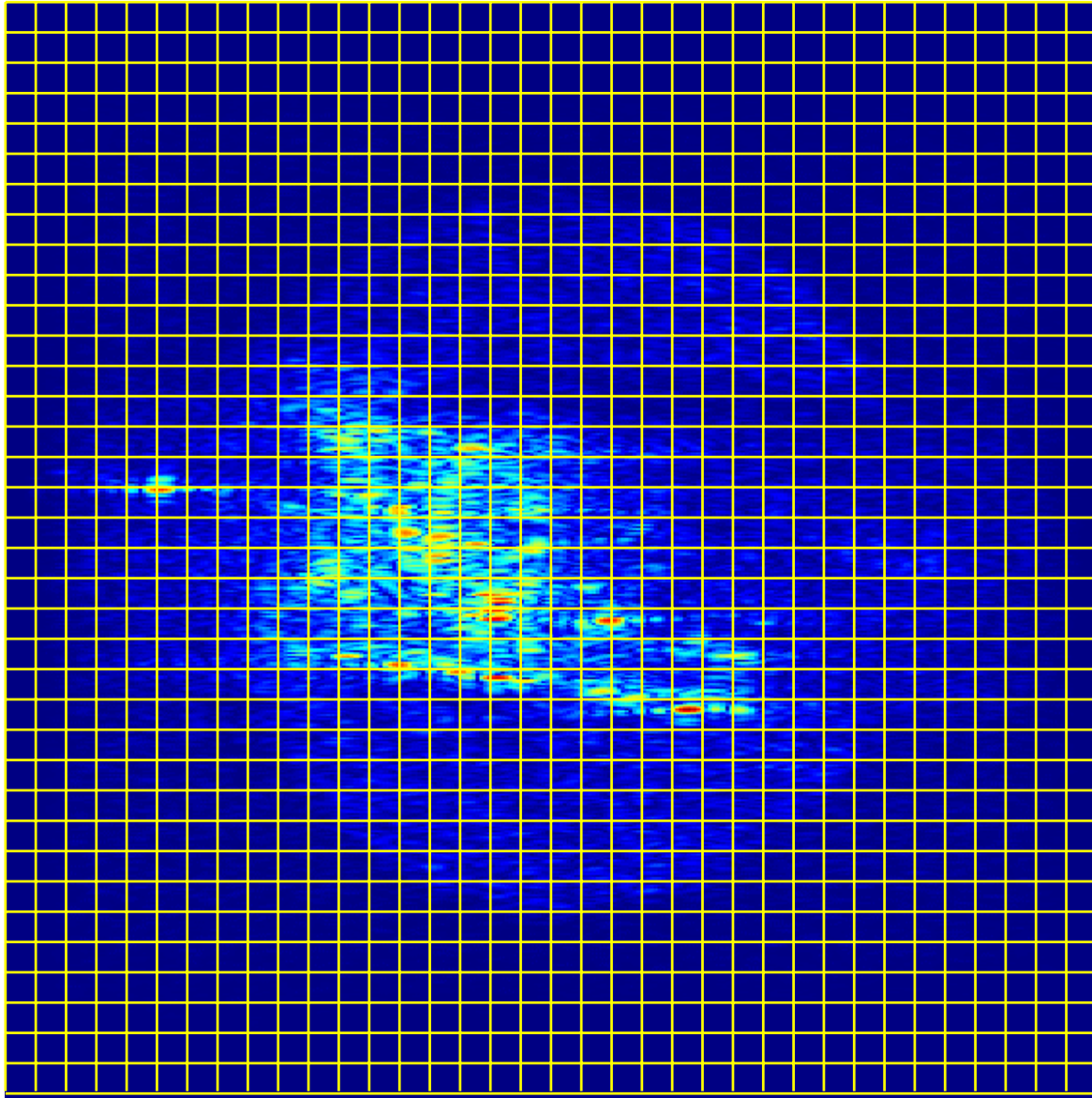
Polar Format Reconstruction: Integration Angle = 32



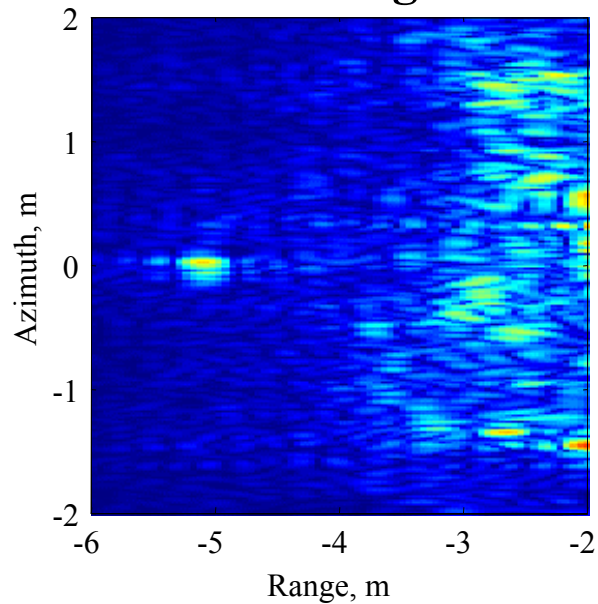
Wavefront CSAR Reconstruction: Integration Angle = 32



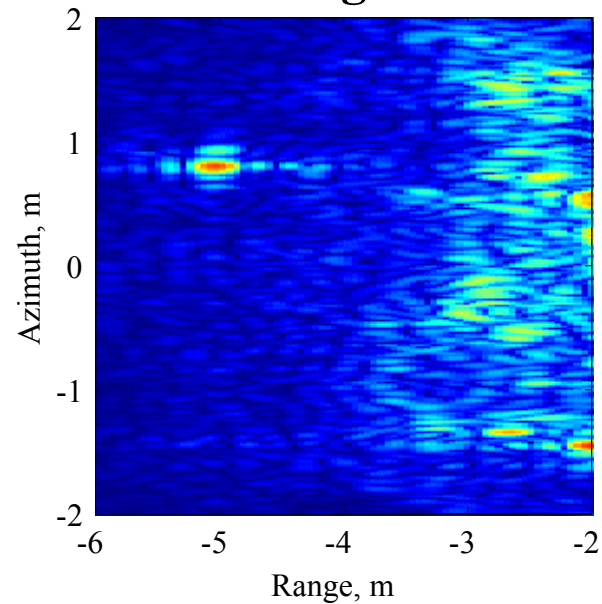
Block Partitioning of Reconstruction



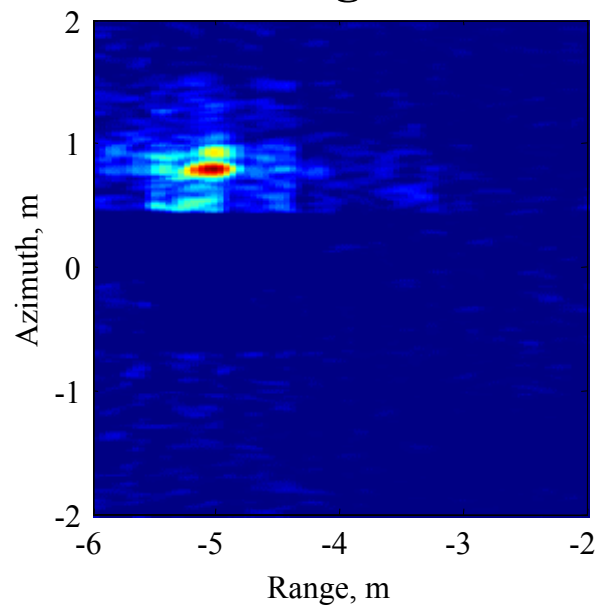
Reference Image: T06



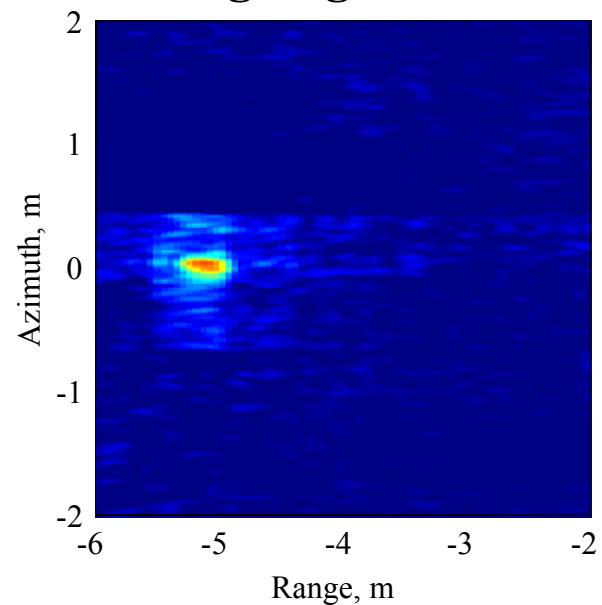
Test Image: T07



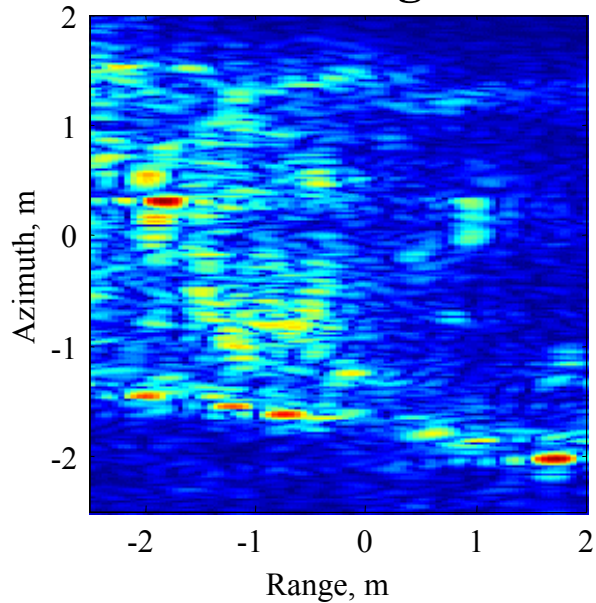
Incoming CSSD



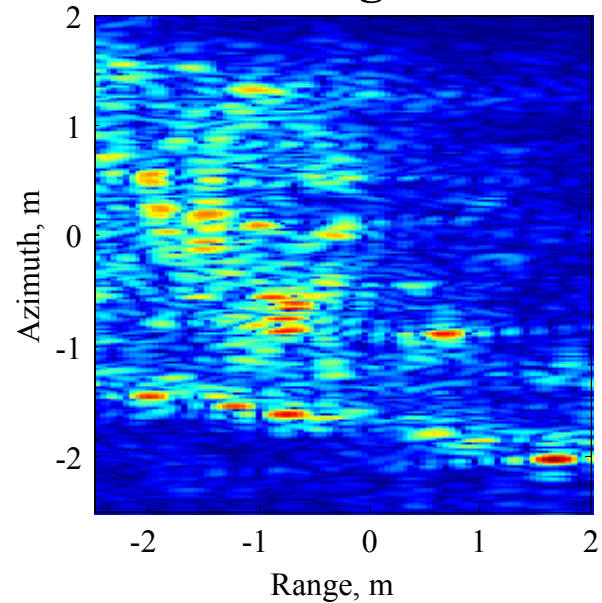
Outgoing CSSD



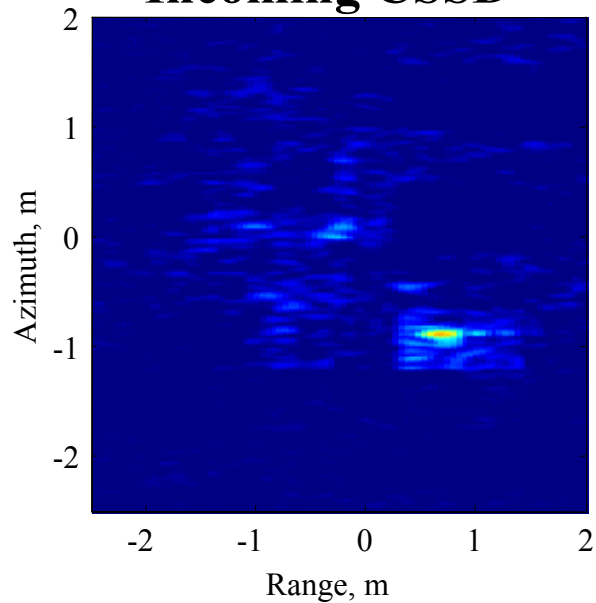
Reference Image: T06



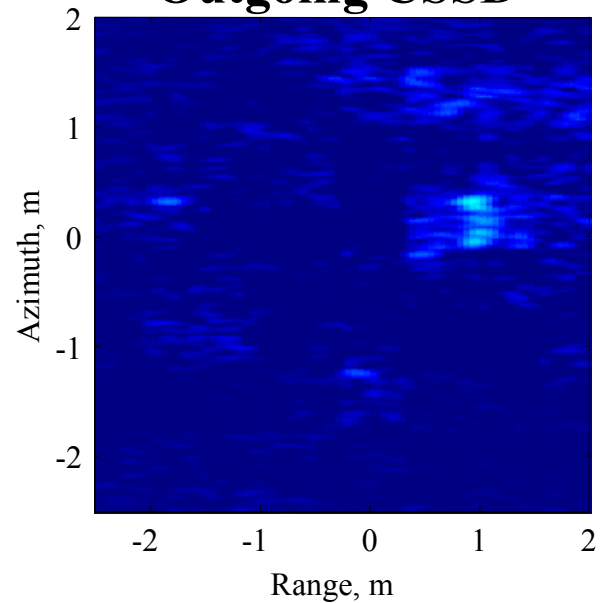
Test Image: T07



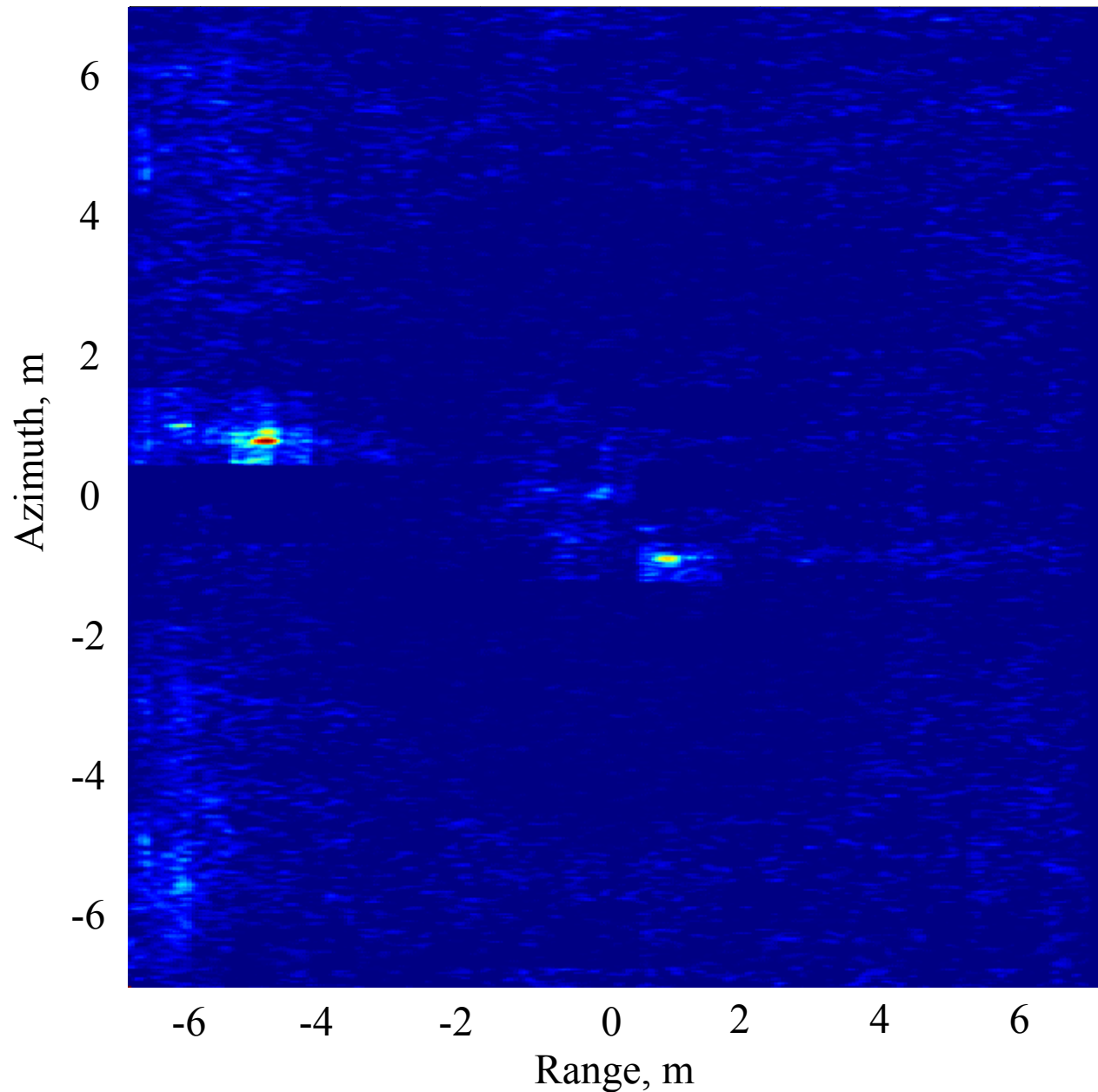
Incoming CSSD



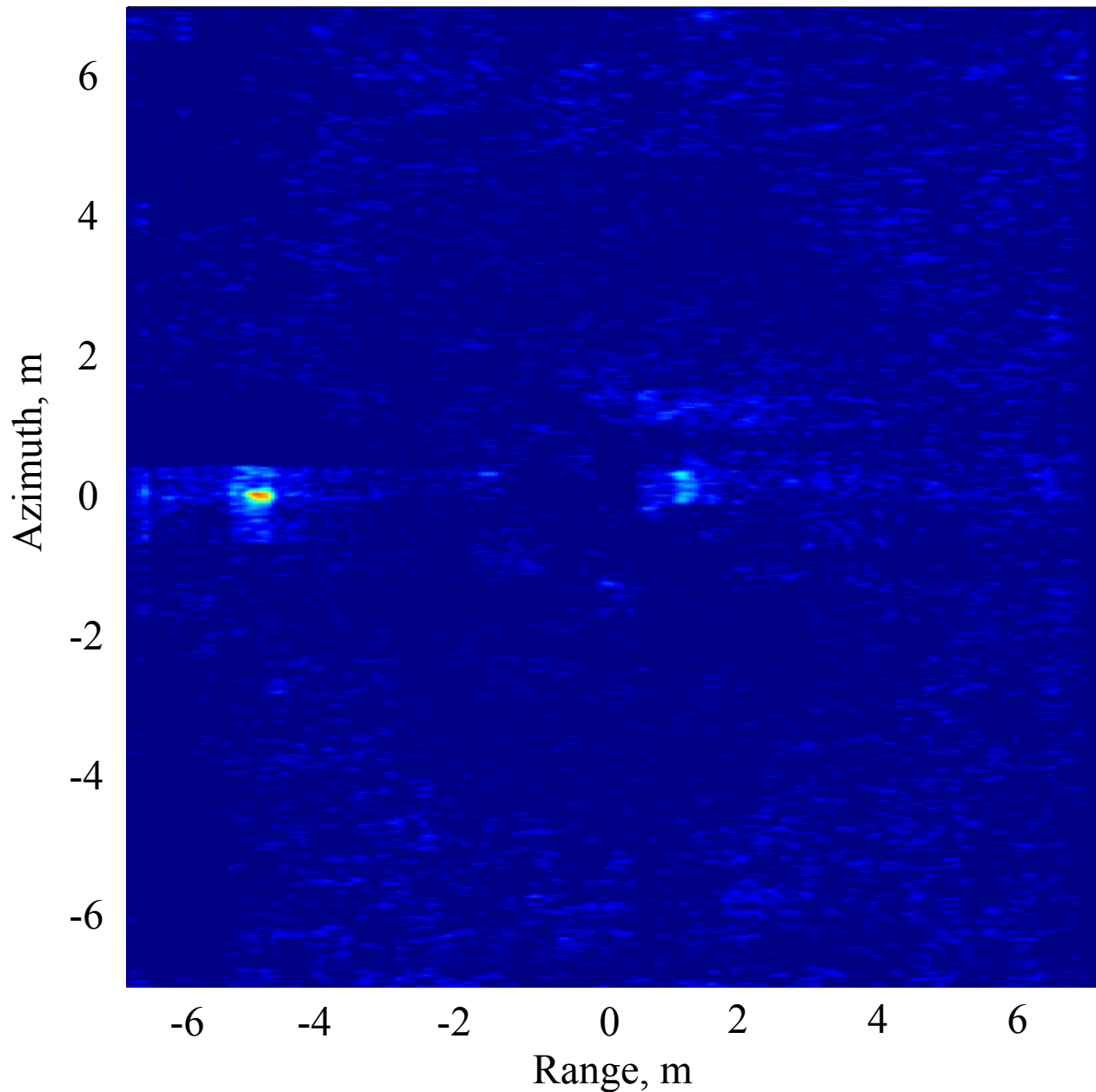
Outgoing CSSD



Incoming Coherent Signal Subspace Difference: T06-T07



Outgoing Coherent Signal Subspace Difference: T06-T07



Summary

- Sensor calibration is a critical problem that has to be dealt with (though ignored) in noncoherent and coherent imaging systems such as SAR
- Simple modification and/or reformulation of existing 1D adaptive (blind) filtering methods exist for 2D calibration problems of SAR-ATR, SAR-Coherent Change Detection (CCD), SAR-MTI, etc.

References

- Soumekh, *SAR Signal Processing*, Wiley, 1999
- Dilsavor, Mitra, Hensel, Soumekh, “GPS-Based Spatial and Spectral Registration of Delta-Heading Multipass SAR Imagery for Coherent Change Detection,” *Proc. U.S. Army Workshop on Synthetic Aperture Radar Technology*, Redstone Arsenal, October 2002
- Soumekh, “Moving Target Detection and Imaging Using an X Band Along-Track Monopulse SAR,” *IEEE Trans. On Aerospace and Electronic Systems*, January 2002
- Soumekh, Himed, “SAR-MTI Processing of Mutli-Channel Airborne Radar Measurement (MCARM) Data,” *Proc. IEEE Radar Conf.*,” May 2002